SOLVATOCHROMIC PYROGALLARENES AND PYROGALLARENE CRYSTALS

A Thesis

presented to

the Faculty of the Graduate School

at the University of Missouri-Columbia

In Partial Fulfillment

of the Requirements for the Degree

Masters of Chemistry

---

by

PAUL D. SPIEL

Dr. Jerry Atwood, Thesis Supervisor

DECEMBER 2018

The undersigned, appointed by the dean of the Graduate School, have examined the Thesis entitled

SOLVATOCHROMIC PYROGALLARENES

AND PYROGALLARENE CRYSTALS

presented by Paul Spiel,

a candidate for the degree of Masters of Science in Chemistry,

and hereby certify that, in their opinion, it is worthy of acceptance.

_____

Professor Jerry Atwood

_____

Professor Kent Gates

_____

Professor Zhen Chen

DEDICATION

To Kinsey and Emery. You bring me life and joy.

ACKNOWLEDGEMENTS

I would like to thank Dr. Atwood for giving me the opportunity to research supramolecular structures. Thank you Dr. Kelley for assisting me in obtaining crystallographic data. Thank you Dr. Wycoff for coaching me on NMR spectroscopy techniques. Thank you Kanishka, Asanka, Kyle, and Durgesh for being a part of the group.

TABLE OF CONTENTS

LIST OF FIGURES

LIST OF TABLES

LIST OF SCHEMES

ABSTRACT

Pyrogallarenes have the ability to self-assemble into a variety of structures. Crystal forms ranging from bilayers to dimers and hexamers have been isolated. One unique cocrystal, $PgC_3 \cdot (CH_3)_2CO \cdot 0.5C_6H_4Cl_2 \cdot nH_2O$, is shown here. This cocrystal of *C*-propyl pyrogallol[4]arene and the pharmaceutical gabapentin has the potential to alter gabapentin's stability, bioavailability, and dissolution rate. During the cocrystallization process unusual chromogenic behavior was observed, which led to the isolation of crystal 1, *C*-propyl pyrogallol[4]arene·3acetone·$3H_2O$. Crystal 1 possessed a visible chromophore, but upon vacuum drying the color was quenched. PXRD of the colorless solid proved that vacuum drying resulted in removal of solvent molecules in the crystal structure, a hallmark of solvatochromism. Titration of *C*-propyl pyrogallol[4]arene over the entire pH range showed that the solvatochromism was pH-sensitive. *C*-propyl pyrogallol[4]arene operates as a pH indicator but is chemically distinct from common pH indicators. Mapping of hydrogen bonding interactions in crystal 1 reveals that water acts primarily as a base in crystal 1, yet the hydroxyl rim is fully protonated. Crystal 2 corroborates solvatochromism found in crystal 1. Finally, solution-phase thermodynamic shifts in absorbance suggest that self-assembly may be traced through solvatochromic interactions. Pyrogallarene solvatochromism is an area that has been previously overlooked but holds great potential to expand understanding of supramolecular structures and self-assembly.

INTRODUCTION

Supramolecular structures have been shown to exhibit an array of potentially useful properties in gas sorption/separation, tube-like assemblies, cocrystallizations, metal-organic frameworks, and molecular encapsulation. Pyrogallol[4]arenes and resorcin[4]arenes are a subset of self-assembling supramolecular macrocyclic compounds. These molecules are equipped with twelve and eight hydroxyl groups at the upper rim, respectively, which can self-assemble into hexamers[1,2] having an internal volume of more than 1,300 $Å^3$.

Metal-organic nanocapsules (MONCs) have been a particular subject of interest in supramolecular chemistry recently. Nanocapsules have been reported with a variety of metals including nickel,[3] magnesium,[4] zinc,[5] cobalt,[6] copper,[7] and gallium.[8] Mixed-metal capsules have also been synthesized, mainly composing gallium and zinc.[8] In and of themselves these complexes are chemically interesting, but they also possess potential as building blocks for metal organic frameworks (MOFS) or as capsules for molecular guests.

Often solvent molecules are encapsulated in supramolecular nanocapsules, but a principle objective is to incorporate active pharmaceutical ingredients (API's) as guest molecules to facilitate targeted drug delivery. On the road to incorporating API's as supramolecular guests is the process of cocrystallizing APIs with supramolecular structures. These structures aid in the elucidation host-guest interactions, a model of fundamental *en vivo* cavity binding, and allow for the preparation of cocrystallized API's with improved properties over the API alone. Through crystal engineering supramolecular structures can facilitate tunable pharmacological properties, improving

API's bioavailability, stability, solubility, and dissolution rates.[9] Gabapentin, a well-known pharmaceutical used in the treatment of epilepsy and neuropathic pain, has been used in such cocrystallization experiments.[10–16] Gabapentin possesses both hydrogen bond donating and accepting sites that work in coordination with the hydrogen bond donating and accepting sites on *C*-propyl pyrogallol[4]arene, making it an ideal candidate for such endeavors.

Although supramolecular interactions are often quantified through single crystal x-ray diffraction, solution-phase interactions of supramolecular structures are of particular interest. Much is still needed to be done in the area of aqueous supramolecular chemistry.[17] Questions abound regarding the solvation of non-polar surfaces and ions, enthalpy-entropy compensation, and how the Hofmeister and hydrophobic effects affect supramolecular self-assembly.[17]

To answer questions about aqueous structures supramolecular chemists often utilize guest probe molecules to monitor shifting NMR absorbance. In other studies fluorescent probes have been used and monitored. These probes are encapsulated as guests in the supramolecular cavity or covalently bonded the macrocycle. UV Vis studies have been performed using the fluorescence of the probes,[18–27] however these studies failed to recognize the chromogenic properties of pyrogallarenes themselves.

In our search to develop new co-crystals of pyrogallarenes solvatochromic behavior was observed and explored, resulting in the discovery that solvatochromism is inherent to pyrogallol[4]arenes alone. Applications of this are 1) pyrogallarenes can be used as solvatochromic pH indicators, 2) pyrogallarenes may be used to assess water

content in hygroscopic solvents, and 3) pyrogallarenes may be used to monitor self-assembly colorimetrically.

Solvatochromism (or, more accurately, perichromism[28]) has been observed and predicted,[29] but much remains unknown about the phenomenon, largely because of the complex set of interactions and dynamic processes that characterize it.[30] Similarly, little is known about the solution structures of complex supramolecular self-assembly.[17,31] Much of what has been discovered regarding solution-phase structures of supramolecular complexes has been obtained through small-angle neutron scattering (SANS), an expensive and arduous process.[31] Solvatochromic studies, such as the work presented here, may help simplify these complex processes and elucidate these interactions.

PYROGALLARENE CO-CRYSTALS

Pyrogallol[4]arenes (Scheme 1) and resorcin[4]arenes are synthesized through a single aldol condensation reaction. ACS-grade reagents are commonly used as pyrogallol or resorcinol are dissolved in methanol or ethanol and an aldehyde is added dropwise to the mixture. A catalytic amount of HCl is then added, and the mixture refluxes for 18 to 24 hours at 90-100°C. Polymer is a side-product of the reaction, and vacuum filtration is undertaken to separate out the colorless pyrogallarene or resorcinarene. Yields have been reported above 90%.[32] Microwave assisted synthesis of pyrogallol[4]arenes and resorcin[4]arenes have been accomplished with maximum yields in n-butanol with an irradiation time of 7 minutes.[32] C-methyl pyrogallol[4]arene (PgC_1) through C-decyl pyrogallol[4]arene (PgC_{12}) are commonly synthesized with aldehydes acetaldehyde through undecanal, respectively. PgC_1 is best synthesized in methanol, but PgC_2 through PgC_{10} appear to react in methanol or ethanol, with ethanol being favored for higher yields. C-propan-3-ol pyrogallol[4]arene (PgC_3OH) and C-butan-4-ol pyrgoallol[4]arene (PgC_4OH) may be synthesized via a ring-opening metathesis involving 2,3-dihydrofuran and 3,4-dihydro-2H-pyran, respectively.[33]

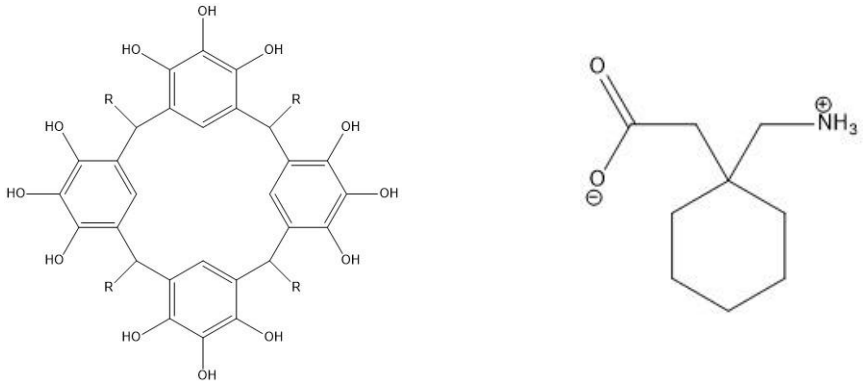

Scheme 1. Structures of PgC_n, n=alkyl tail length (left) and gabapentin (right).

To form co-crystal **1** gabapentin and PgC_3 (Fig. 1) were weighed out in a 2:1 molar ratio, respectively, and dissolved in a 1:1 by volume solution of acetone and water. Approximately 50 µL of 1,2-dichlorobenzene were added to the solution followed by sonication at 40°C. After sonicating the solution transformed from clear to a brilliant magenta. Colorless crystals were collected following two days of room temperature evaporation.

The single crystal X-ray diffraction data for cocrystal **1** were collected on a Bruker D8 Venture diffractometer equipped with a Photon 100 CMOS area detector using MoKα radiation (0.71073 Å) from a microfocus source. The crystal was cooled to 100K under a stream of cold N_2 using an Oxford Cryosystems Cryostream 800 cryostat. A hemisphere of unique data was collected using a strategy of shutterless scans about the omega and phi axes. Unit cell determination, data collection, data reduction, absorption correction, and scaline were performed using the Bruker Apex3 software suite.

The crystal structure of **1** was solved by direct methods and refined by full matrix least squares refinement against F^2. Non-hydrogen atoms associated with the PgC_3, acetone, and gabapentin moieties and a single unique chlorine atom of the dichlorobenzene moiety were located from the difference map and refined anisotroptically. The position of the chlorine atom indicated that the dichlorobenzene molecule was disordered about a crystallographic inversion center such that the two chlorine atoms were present in defined positions at 100% occupancy, while the carbon atoms were disordered on either side of the inversion center at 50% occupancy. A number of significant electron density peaks appeared around the carbon atoms of the dichlorobenzene moiety, most likely indicating other orientations which could not be

completely resolved. The contribution of disordered molecules in the lattice was removed from F_{obs} using the program PLATON SQUEEZE.[34] Structure solution and refinement were conducted using SHELXL-2014[35] as implemented in Olex2.[36] Molecular graphics were generated with Olex2 or Mercury from the CCDC.[37]

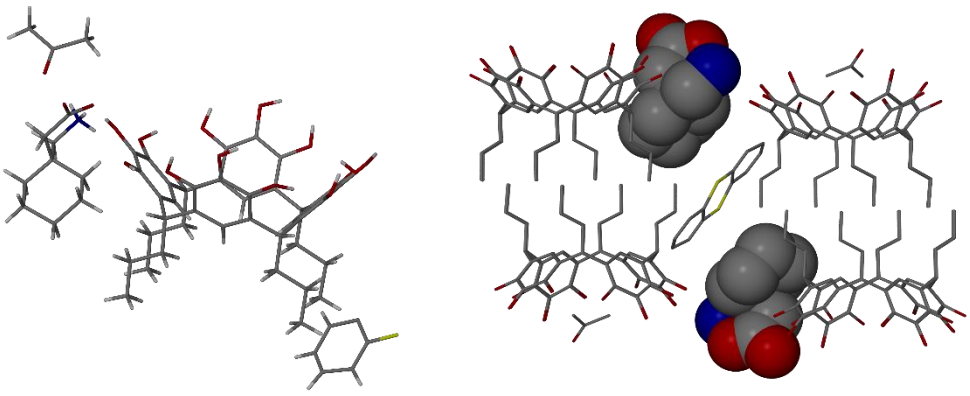

Figure 1. (Left) Single XRD structure for the asymmetric unit of C-propyl pyrogallol[4]arene and gabapentin, cocrystal **1**. (Right) The bilayer packing illustration of cocrystal **1** with space-filled models for the gabapentin molecules. The 1,2-dichlorobenzene molecule is disordered over a crystallographic center of inversion located between the two chlorines, resulting in one chlorine molecule omitted from (a) and one excess 1,2-dichlorobenzene molecule in (b). For clarity hydrogen atoms and solvent molecules have been removed. O: red, C: grey, N: blue, Cl: yellow.

Cocrystal **1** (Fig. 1, Table 1) crystallized in the space group P-1. The formula unit for cocrystal **1** includes one gabapentin molecule, one PgC_3 molecule, one acetone molecule, one-half of a disordered 1,2-dicholorobenzene molecule, and approximately five water molecules. The water molecules were disordered, so they could not be accurately modelled and were removed with SQUEEZE. The 1,2-dichlorobenzene molecule is disordered over a crystallographic center of inversion located between the two chlorines, resulting in one 1,2-dichlorobenzene molecule per two gabapentin formula units. Gabapentin possesses the pH-dependent property of intramolecular hydrogen bonding and is often cocrystallized in its zwitterionic form, as it is presented here. Thus,

the protonated amino group of gabapentin donates one intramolecular hydrogen bond to the gabapentin carboxylate group (N···O, 1.79 Å, 173.6°). In this work, conventional N-H···O and O-H···O interactions are considered H-bonds when the X···O distance is <3.6 Å. Unconventional C-H···O interactions are considered H-bonds when the C···O distance is <3.9 Å. In all cases, the X-H···O angle must be greater than 90°.[38–40]

Table 1. Crystal data and structure refinement for PgC3·acetone·0.5C6H4Cl2·nH2O		
Empirical formula	C55 H73 Cl N O15	
Formula weight	1023.59	
Temperature	100.0 K	
Wavelength	0.71073 Å	
Crystal system	Triclinic	
Space group	P-1	
Unit cell dimensions	a = 11.7633(9) Å	α= 71.988(2)°.
	b = 15.6968(12) Å	β= 82.735(3)°.
	c = 17.8554(14) Å	γ = 71.812(3)°.
Volume	2977.1(4) $Å^3$	
Z	2	
Density (calculated)	1.142 Mg/m^3	
Absorption coefficient	0.125 mm^{-1}	
F(000)	1094	
Crystal size	0.35 x 0.12 x 0.08 mm^3	
Theta range for data collection	2.216 to 26.655°.	
Index ranges	-14<=h<=12, -19<=k<=19, -22<=l<=22	
Reflections collected	85963	
Independent reflections	12406 [R(int) = 0.1350]	
Completeness to theta = 25.242°	99.9 %	
Absorption correction	Semi-empirical from equivalents	
Max. and min. transmission	0.7454 and 0.6362	
Refinement method	Full-matrix least-squares on	

	F^2	
Data / restraints / parameters	12406 / 542 / 697	
Goodness-of-fit on F^2	1.037	
Final R indices [I>2sigma(I)]	R1 = 0.0968, wR2 = 0.2366	
R indices (all data)	R1 = 0.1560, wR2 = 0.2730	
Largest diff. peak and hole	2.515 and -0.906 e.Å^{-3}	

The acetone molecule of cocrystal **1** is located above the cavity of the PgC_3 structure and is adjacent to the gabapentin molecule. One of the methyl groups of the acetone has a C-H···π interaction with the lower rim of the PgC_3 bowl of (2.83 Å) and the other methyl has two C-H···π interactions with the lower rim of the PgC_3 bowl of (2.76 Å and 2.88 Å). In our previous report[16] the acetone molecule sitting in the cavity of the PgC_3 molecule was orientated such that only one methyl group interacted with the π electrons of the PgC_3 structure. The carbonyl of the acetone in cocrystal **1** hydrogen

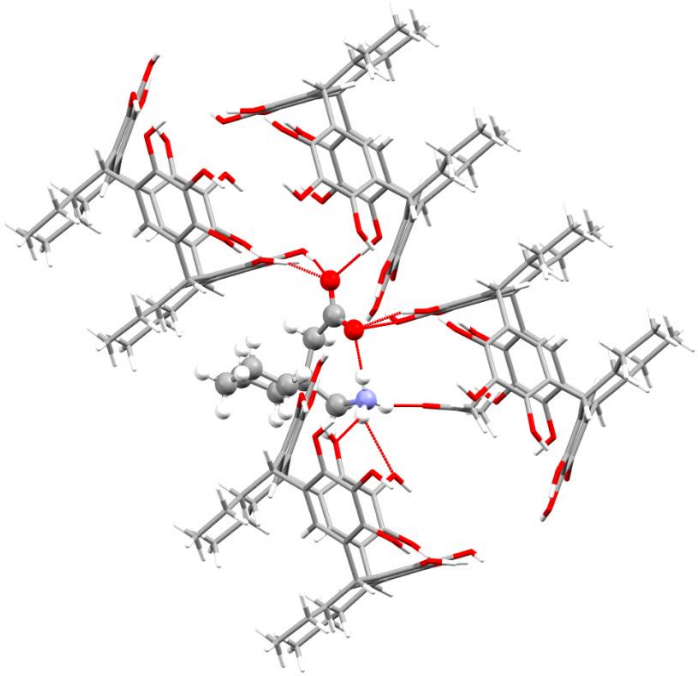

Figure 2. The H-bonding interactions of gabapentin with other components of the cocrystal (indicated as lines).

bonds with the amine group of gabapentin (2.81 Å, 164.1°) and also hydrogen bonds with the upper rim of an adjacent PgC_3 molecule (2.93 Å, 144.7°).

We have previously reported PgC:gabapentin cocrystallizations with macrocycle-to-pharmaceutical ratios of 1:1 and 1:2, respectively.[16,41] In these structures, gabapentin has been crystallized *exo* and *endo* with respect to the macrocyclic cavity.[16,41] In each case of *endo* positioning the gabapentin is crystallized near the upper rim of the macrocyclic cavity, not in the alkyl tails of the macrocycle.

The gabapentin molecule in cocrystal **1** resides *exo* to the macrocyclic cavity and, in addition to intramolecular bonding and hydrogen bonding with the acetone molecule discussed earlier, it interacts with three adjacent PgC_3 molecules. The amine group of gabapentin hydrogen bonds with an adjacent PgC_3 hydroxyl tail (N-H···O, 2.82 Å, 160.7°). The carbonyl group also interacts with two adjacent PgC_3 hydroxyl tails (O···H, 2.66 Å, 173.5° and 2.67, 156.1°). We have previously reported only one cocrystal where a gabapentin was not *endo* to the macrocyclic cavity.[16] In that case two *exo* gabapentin molecules resided as a dimer in the asymmetric unit, hydrogen bonding with each other and with the hydroxyl tails on the upper rim of the macrocyclic bowl.[16] However, cocrystal **1** only possesses one gabapentin molecule *exo* to the macrocyclic bowl. This gabapentin molecule hydrogen bonds with several PgC_3 molecules and does not hydrogen bond with another gabapentin molecule.

Previously it was reported that adding drops of nitrobenzene or 1,2-dicholorbenzene to a solution of PgC_3 facilitated the crystallization of hexameric molecular capsules.[42] To that end drops of 1,2-dicholorbenzene were added to the solution of milligram quantities of gabapentin and PgC_3. The original proposition for the

formation of hexameric molecular capsules upon the addition of a polar benzene entity was that the benzene entity prevented the formation of too many nucleation sites, leading to the formation of microcrystals.[42] However, the cocrystal presented herein suggests that 1,2-dichlorobenzene can sometimes participate in the cocrystallization of a PgC_3 bilayer. These results indicate that there are yet undiscovered cocrystallizations of gabapentin and

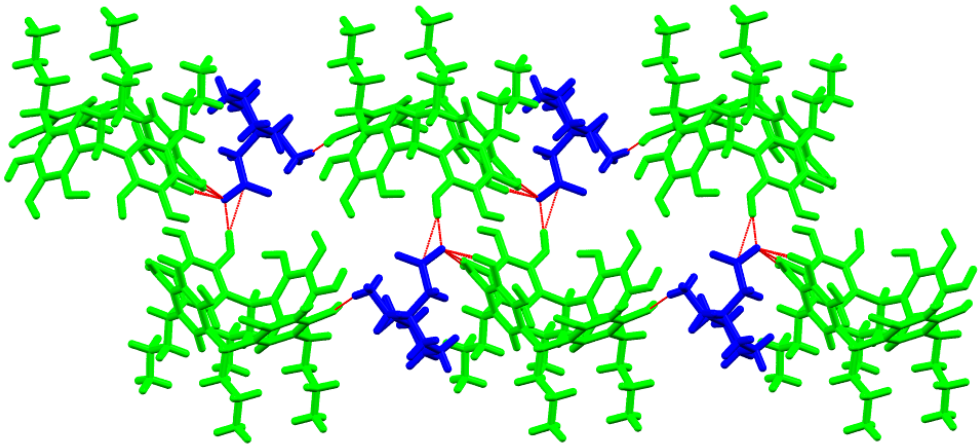

Figure 3 Packing plot showing bilayer of cocrystal **1**. As discussed earlier, the gabapentin molecule hydrogen bonds with the hydroxyl tails of the adjacent PgC_3 molecules. Atoms have been color coded by molecule for clarity (green = PgC_3, blue = gabapentin). Hydrogen bonds shown as red lines.

pyrogallol[4]arenes. Slight modifications in the solvent system can lead to large changes in cocrystallized structure. These variables may be manipulated to achieve the desired properties of the API.

Gabapentin cocrystallizations vary in location and interaction with pyrogallol[4]arenes. The gabapentin molecule can be crystallized *exo* or *endo* to the macrocyclic cavity, in a dimeric or monomeric form. In all cases these cocrystals are formed in protic solvents, often a 50:50 mixture of acetone and water, but small changes in solvent system or macrocyclic framework can result in varied properties of the macrocyclic cocyrstallization. In this paper we have described a cocrystallization of

gabapentin and *C*-propyl pyrogallol[4]arene that incorporates a symmetrically disordered 1,2-dichlorobenzene molecule. The results of this cocrystallization further develop the crystal engineering of tuneable API's.

PYROGALLARANE SOLVATOCHROMISM

Supramolecular structures are often crystallized without purity in mind, as impurities provide nucleation sites for crystallization. Nevertheless, in previous work I embarked upon the process of creating a substantially pure *C*-propyl pyrogallol[4]arene (PgC_3) solution in acetone and water and observed the occurrence of a visible magenta in solution. The crystals obtained in the previous work were colorless, and the color in solution largely could have been attributed to an unknown purity. Nonetheless the chromogenic properties were examined and pursued.

Exploring the magenta color shift led me to recognize that the color shift from clear to magenta occurred in additional solvents, namely DMSO, DMF, Acetone, and Acetone/Water mixtures. The pyrogallol[4]arene solid was further purified, yet the colorless organic reagents produced a colored solution. Since multiple crystal forms may nucleate out of the same solution, the crystallization parameters were varied to isolate the chromogenic structure.

In order to capture a chromogenic crystal the crystallization process had to be expedited, since the desired color shift was lost over a period of time. Selectively crystallizing out colored crystals would require atmospheric or expedited evaporation. Atmospheric evaporation was attempted by modulating partial vapor pressures, but it did not produce crystals in a sufficient time frame. Subsequently expedited evaporation was attempted by blowing a gentle stream of compressed air on the solution for a period of 18 to 24 hours.

Through subsequent iterations I was able to selectively crystallize out the chromogenic structure, Crystal **1**, *C*-propyl pyrogallol[4]arene·3acetone·3H_2O (Fig. 4). This crystal has since been reproduced multiple times.

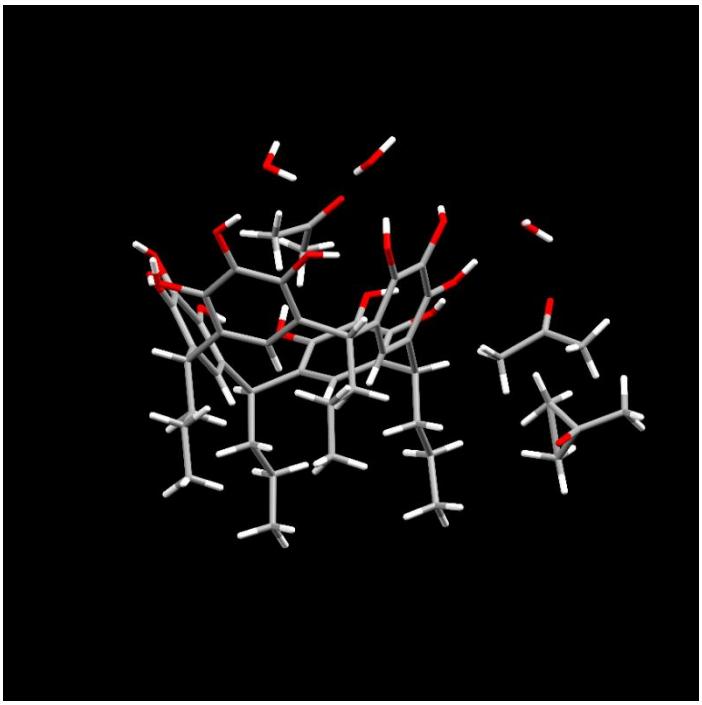

Figure 4. Crystal **1**, possessing one C-propyl pyrogallol[4]arene, three ordered water molecules, and three acetone molecules.

Since Crystal **1** possessed the same magenta color as the solution with a UV_{max} of 509 and did not contain any chromophoric guests it was assumed that the colors of the solution were the result of the pyrogallol[4]arene interactions with the solvent molecules of the crystal, water and acetone. This could not be definitively concluded, as impurities on the crystal could be responsible for its chromogenic properties. However, after placing single crystals of Crystal **1** in a vacuum dryer overnight the crystal color disappeared. Single XRD was attempted on the crystals, but did the crystals did not provide a sufficient diffraction pattern, suggesting that the asymmetric unit cell was disrupted.

Powder X-Ray Diffraction (PXRD) was subsequently performed on the colored crystal and colorless solid, shown in Figure 5.

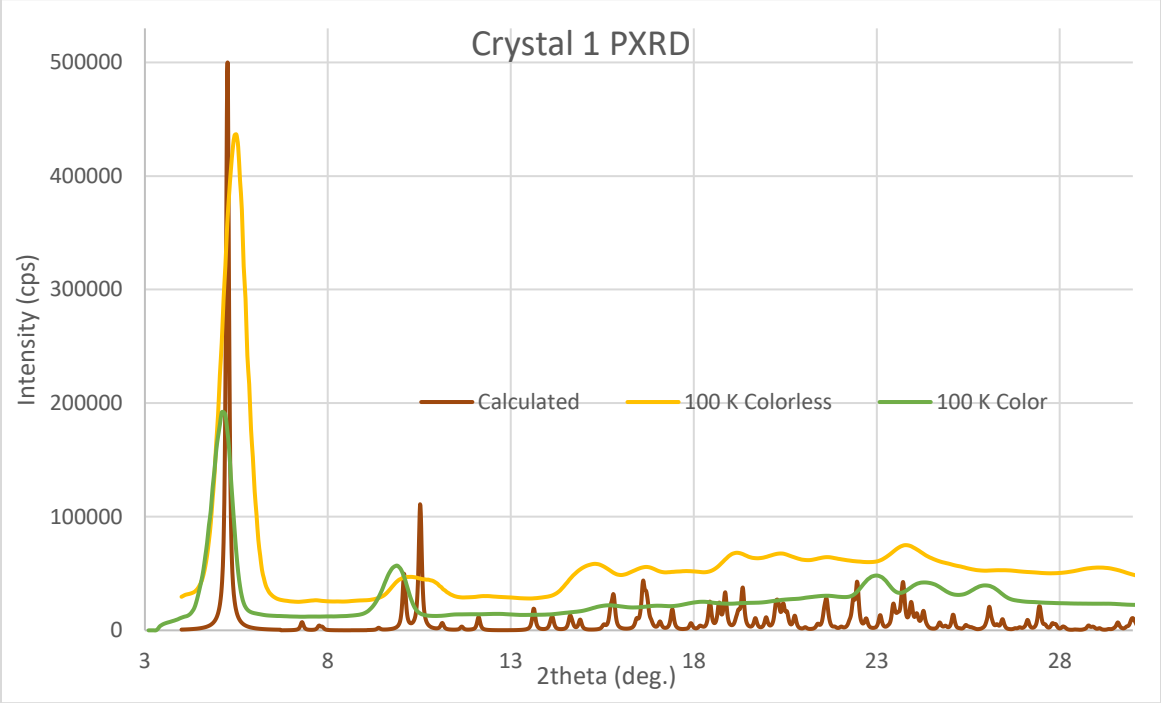

Figure 5. PXRD data from colorless and colored samples of Crystal **1**. The lowest angle peak shows compression along the *C* axis.

Figure 5 shows that the colorless powder is isostructural with Crystal **1**. However, the colorless peaks indicate important shifts when compared to the colored and calculated peaks. The lowest angle peak, which corresponds to the (0,0,1) peak of the single crystal, is shifted to a slightly higher angle. This indicates a decrease in the length of the *C* axis upon drying. See Figure 6 for Crystal **1** axes. This data is consistent with the removal of solvent molecules from the crystal structure as acetone and water form layers that separate the *C*-propyl pyrogallol[4]arenes along the *C* axis. This directly indicated that that the color change was correlated with a change in the intermolecular environment of the pyrogallarenes in the crystal structure, a hallmark of solvatochromism.

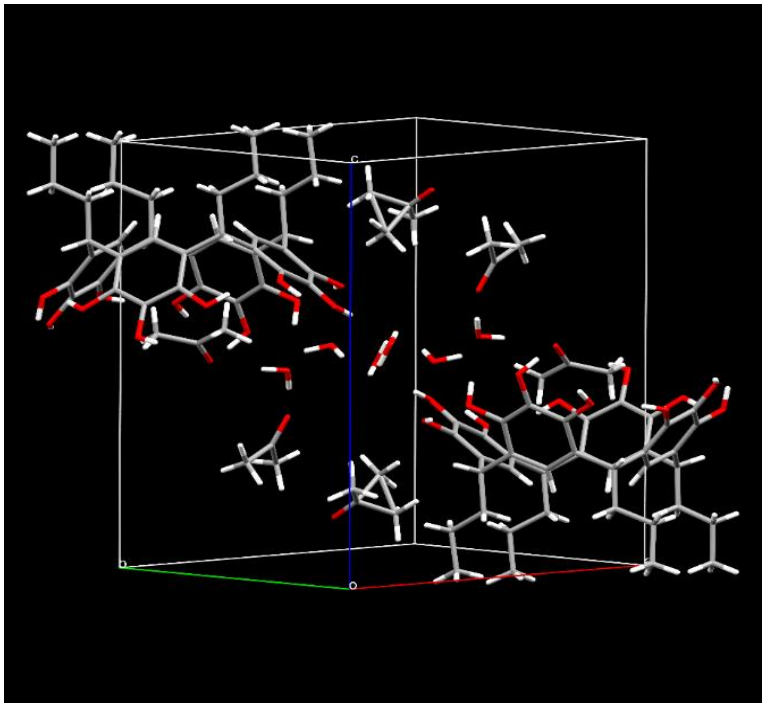

Figure 6. Axes of Crystal **1**. The *C* axis, the distance between the pyrogallol[4]arene rims, is shown vertically and represented in blue.

To fully understand the solvatochromic behavior of pyrogallarenes a series of experiments were performed. First, I analyzed the solvatochromic behavior of pyrogallarenes in the presence of various acids and bases. Strong bases of NaOH and NH_4OH greatly amplified a magenta color, and strong acids quenched the color or produced a yellow, depending upon the pyrogallol[4]arene concentration. Upon titrating pyrogallol[4]arenes over the entire pH range I observed an abrupt color change in the range of pH 4.5 to 6, demonstrating the usefulness of *C*-propyl pyrogallol[4]arene as a pH indicator.

In order to determine whether the hydrocarbon tail of various pyrogallarenes affected chromogenic behavior several pyrogallarene structures were examined. I investigated *C*-methyl pyrogallol[4]arene, *C*-ethyl pyrogallol[4]arene, *C*-propan-3-ol

pyrogallol[4]arene, *C*-butyl pyrogallol[4]arene, *C*-hexyl pyrogallol[4]arene, *C*-heptyl pyrogallol[4]arene, and *C*-decyl pyrogallol[4]arene in acidic and basic environments and found consistent results with those of *C*-propyl pyrogallol[4]arene. At a high pH the structures exhibit a pink/magenta color, and at a low pH a colorless or yellow color prevails. This indicates that the hydrocarbon tails do not greatly affect the solvatochromic interactions, and the hydroxyl rim is mainly responsible for the pH-dependent solvatochromic behavior.

Pyrogallol[4]arenes are unexpected candidates as pH indicators as they are chemically distinct from traditional pH indicators. This gives reasoning, in addition to the crystallographic data, to suggest that pyrogallol[4]arene chromogenic properties likely come from solvatochromism. Unlike common pH indicators (see Table 2), the deprotonation of a hydroxyl group on the pyrogallol[4]arene upper rim does not unlock and expand a highly conjugated pi system. Although the adjacent phenol groups of the pyrogallol[4]arene can hydrogen bond with each other, the aromatic rings are isolated from each other because they lack a connecting sp^2 carbon.

Table 1Table 2 - Common Indicators	
Phenolphthalein	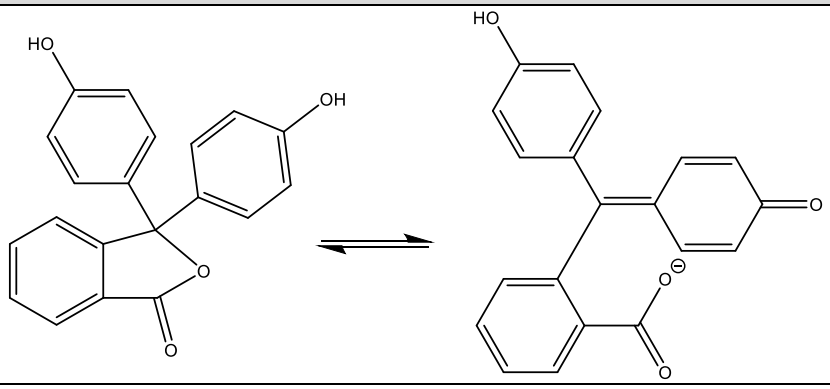

Bromocresol green	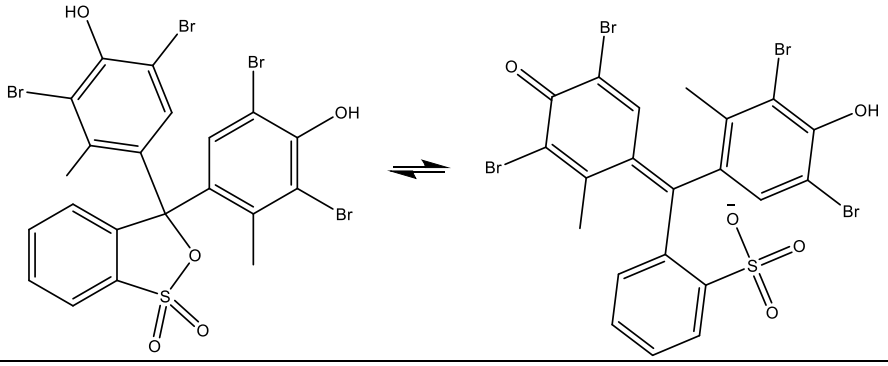
Bromothymol blue	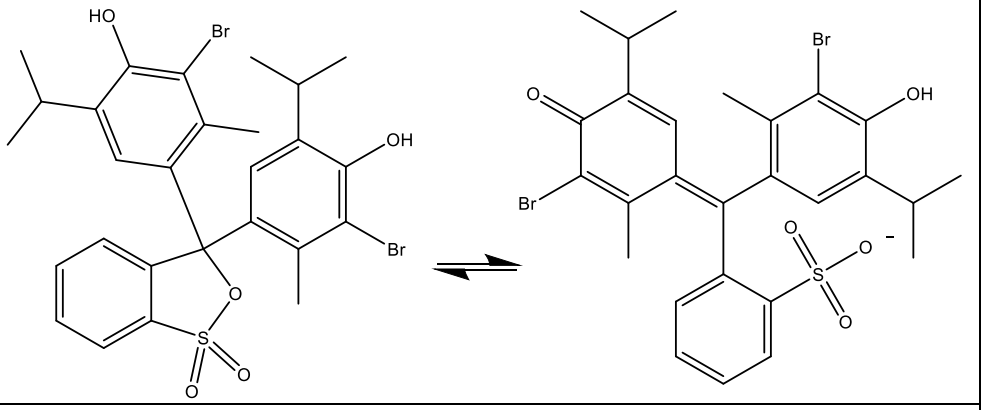
Methyl orange	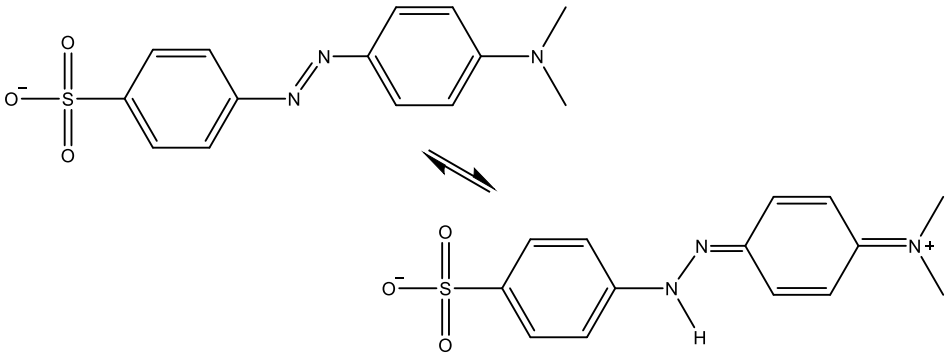

As shown in Table 2, phenolphthalein, bromocresol green, and bromothymol blue operate via the expansion and contraction of a highly conjugate pi system. Protonation and deprotonation results in the HOMO and LUMO bandgap of these molecules being shifted from outside of the visible spectrum to the visible spectrum. Similar indicators not shown in Table 1, such as bromocresol purple, phenol red, naphtholphthalein, cresol red,

o-cresolphthalein, thymolphthalein, malachite green, thymol blue, chlorophenol red, brilliant yellow, curcumin, metacresol purple, and p-naptholbenzein operate similarly with the expansion or contraction of a highly conjugated pi system via the protonation or deprotonation of the molecule.

Methyl orange and other benzidine derived dyes (such as congo red, methyl red, methyl yellow, propyl red, ethyl red, ethyl orange, dimethyl yellow) are a slight exception to this trend. Upon protonation of the molecule the nitrogen adds a proton, but the azo nitrogen retains some sp^2 character and does not fully convert to an sp^3 hybridized orbital. Thus, the molecule's conjugation mostly continues through the azo bond, as the protonated azo nitrogen does not have full sp^3 character.

Interestingly, most organic solvatochromic molecules possess at least two aromatic rings in conjugation with each other, a trait that pyrogallarenes do not possess. In a chemical review Reichardt[29] identified seventy-six molecules that exhibit solvatochromism. Of the organic solvatochromic molecules identified, only two contain fewer than four conjugated double bonds, and only ten do not have two aromatic rings in conjugation with each other. In addition to the seventy-six molecules identified, Reichardt[29] predicted that other polycyclic aromatic hydrocarbons would be solvatochromic. Polyaromaticity is something that pyrogallarenes lack, and solvatochromism would not be predicted off of this molecular trend.

Ultimately, any shift in absorbance is a result of energy changes in the excitation gap between the highest occupied molecular orbital (HOMO) and lowest unoccupied molecular orbital (LUMO) of the indicating molecule. These shifts may be a result of intramolecular changes or intermolecular changes. For common pH indicators shifts in

the HOMO and LUMO result upon protonation or deprotonation of the most reactive acidic site in the molecule.

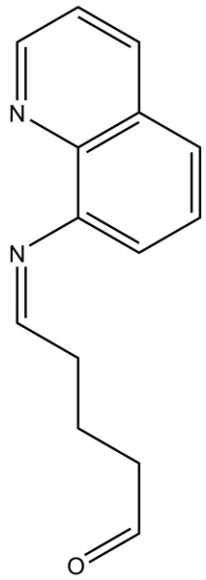

Scheme 2. Solvatochromic indicator 5-(quinolin-8-yliminol) pentanal (QYP).

In addition to this thesis at least one other solvatochromic pH indicator has been reported, namely 5-(quinolin-8-yliminol) pentanal (QYP) (Scheme 2).[43] In their report they concluded that QYP's colorimetric response depended on the change of pH values rather than the reaction of QYP with the ions in buffered solutions. Similarly, we believe the pyrogallol[4]arene phenol's interaction with ions is not the cause of the solvatochromic behavior. Irrespective of which acid or base is used the absorption is the same. The absorption is almost strictly dependent upon the pH of the solution. As such, we believe the deprotonated phenol contributes electron density to the pyrogallol[4]arene and increases the solvatochromic interactions already present on the rim of the pyrogallol[4]arene.

In order to corroborate our previous results we sought to isolate another solvatochromic crystal. In time we identified Crystal **2** (Fig. 7), possessing a structure of one *C*-ethyl pyrogallol[4]arene, one acetone molecule, and a number of water molecules, including five ordered water molecules and eight disordered water molecules. As with Crystal **1**, Crystal **2**'s color is quenched upon vacuum drying.

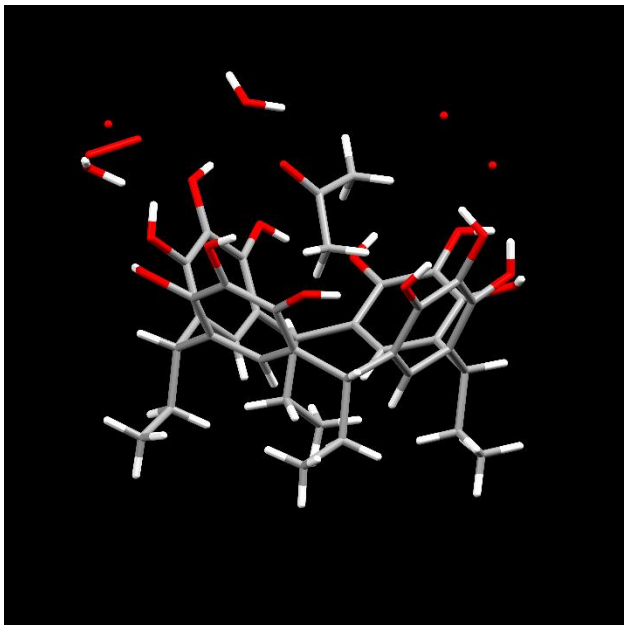

Figure 7. Crystal **2**, crystallized from *C*-ethyl pyrogallol[4]arene.

Crystal **1** and Crystal **2** show several similarities. Both contain an acetone molecule *endo* to the cavity, although in slightly different orientations, and both have water molecules and an acetone molecule hydrogen bonding with the phenol groups of the macrocycle. However, the interactions are not identical. Crystal **1** possesses a finite set of water molecules and a high degree of order. Crystal **2** possesses several more water molecules and much more disorder. In order to fully understand the differences in the hydrogen bonding between the two crystals we mapped out their interactions, shown in Table 3 and Table 4.

Table 1Table 3 - Hydrogen Bonding Interactions of Crystal **1**, $PgC_3 \cdot 3acetone \cdot 3H_2O$.			
O1···O7	PgC	Donates	2.817(1)
O1···O12	Intramolecular	Accepts	2.729(2)
O2···O1W	H_2O	Donates	2.755(2)
O3···O10	PgC	Donates; bifurcated	2.932(2)
O3···O4	Intramolecular	Donates; bifurcated	2.886(2)
O4···O10	PgC	Accepts	2.894(2)
O4···O2W	H_2O	Donates	2.691(1)
O4···O3	Intramolecular	Accepts	2.886(2)
O5···O8	PgC	Donates	2.834(1)
O5···O3W	H_2O	Donates; weak	2.860(2)
O5···O2W	H_2O	Accepts	2.925(1)
O5···O3W	H_2O	Accepts	3.045(1)
O6···O3W	H_2O	Donates	2.663(2)
O6···O7	Intramolecular	Accepts	2.682(2)
O7···O1	PgC	Accepts	2.817(1)
O7···O6	Intramolecular	Donates	2.682(2)
O8···O1S	Acetone	Donates	2.691(2)
O8···O5	PgC	Accepts	2.834(1)
O9···O3W	H_2O	Donates	2.748(1)
O9···C6S	Acetone	Accepts	3.414(2)
O9···O10	Intramolecular	Accepts	2.748(2)
O10···O3	PgC	Accepts	2.932(2)
O10···O4	PgC	Donates, weak	2.894(2)
O10···O9	Intramolecular	Donates	2.748(2)
O11···O2W	H_2O	Donates	2.678(2)
O11···O1W	H_2O	Accepts	3.127(1)
O11···O1W	H_2O	Accepts	2.998(2)
O12···O2W	H_2O	Accepts	2.783(1)
O12···C5S	Acetone	Accepts	3.413(3)
O12···O1	Intramolecular	Donates	2.729(2)

Table 3 shows that Crystal **1** possesses four intramolecular hydrogen bonds, four hydrogen bond donor/acceptor pairs with PgC, five hydrogen bonds are accepted from water, six hydrogen bonds are donated to water (5 strong, 1 weak), and one hydrogen bond is donated to acetone.

Table 4 – Hydrogen Bonding Interactions of Crystal **2**, $PgC_2 \cdot 1$ acetone$\cdot 6\ H_2O$			
O1···O12	Intramolecular	Donates	2.723(4)
O2···O5W	H_2O	Donates	2.712(3)
O2···O4W	H_2O	Accepts	2.917(4)
O2···O8	PgC	Accepts	3.033(3)
O3···O2W	H_2O	Donates; bifurcated	2.821(9)
O3···O3W	H_2O	Donates; bifurcated	3.608(7)
O3···O10	PgC	Accepts	3.094(3)
O3···O4	Intramolecular	Accepts	2.790(3)
O4···O9	PgC	Donates	2.981(3)
O4···O3W	H_2O	Accepts	2.975(8)
O4···O3	Intramolecular	Donates	2.790(3)
O5···O6W	H_2O	Donates	2.699(3)
O5···O3W	H_2O	Accepts	2.975(3)
O6···O12	PgC	Accepts	2.655(3)
O6···O7	Intramolecular	Donates	2.653(3)
O7···O5W	H_2O	Donates	2.670(3)
O7···O6	Intramolecular	Accepts	2.653(3)
O8···O1S	Acetone	Donates	2.724(4)
O8···O2	PgC	Donates; weak	3.033(3)
O8···O2W	H_2O	Accepts	2.92(1)
O8···O3W	H_2O	Accepts	2.845(6)
O9···O1W	H_2O	Donates	2.740(6)
O9···O2W	H_2O	Donates; weak	2.803(8)
O9···O4	PgC	Accepts	2.981(3)
O9···O10	Intramolecular	Accepts	2.784(3)
O10···O3	PgC	Donates; weak	3.094(3)
O10···O9	Intramolecular	Accepts	2.784(3)
O11···O4W	H_2O	Donates	2.672(4)
O11···O6W	H_2O	Accepts	2.881(3)
O12···O6	PgC	Donates	2.655(3)
O12···O1	Intramolecular	Accepts	2.723(4)

Table 4 shows Crystal **2** possesses four strong intramolecular hydrogen bonds, four hydrogen bond donor/acceptor pairs with PgC (two weak), at least six hydrogen bonds are accepted from water, eight hydrogen bonds are donated to water (five strong, two bifurcated, one weak), and one hydrogen bond is donated to acetone.

In total, the hydrogen bonds donated to water are shorter than the hydrogen bonds accepted from water in both Crystal **1** and Crystal **2**. This suggests that water interacts with PgC predominantly as a base in both crystals.

One interesting aspect of pyrogallarene solvatochromism is the growth and attenuation of absorbance patterns. *C*-propyl pyrogallol[4]arenes dissolved in a 50/50 v/v solution of acetone/water exhibits a brilliant magenta color three hours after dissolution. The magenta color grows over a period of hours, but after a period of days the absorption shifts to a yellow color (Fig. 8). Similarly, *C*-propyl pyrogallol[4]arene dissolved in in DMSO, DMF, HPLC acetone, basic solutions, acidic solutions, and other organic solvents or mixtures exhibit this shift over a period of days or weeks, depending upon the solution. Originally it was proposed that C-propyl pyrogallol[4]arene reacted with an impurity or a solvent molecule to cause such a shift in color. However, after taking NMRs of C-propyl pyrogallol[4]arene dissolved in DMSO and acetone/water mixtures (see Appendix) it was evident that the molecule was largely unchanged throughout these

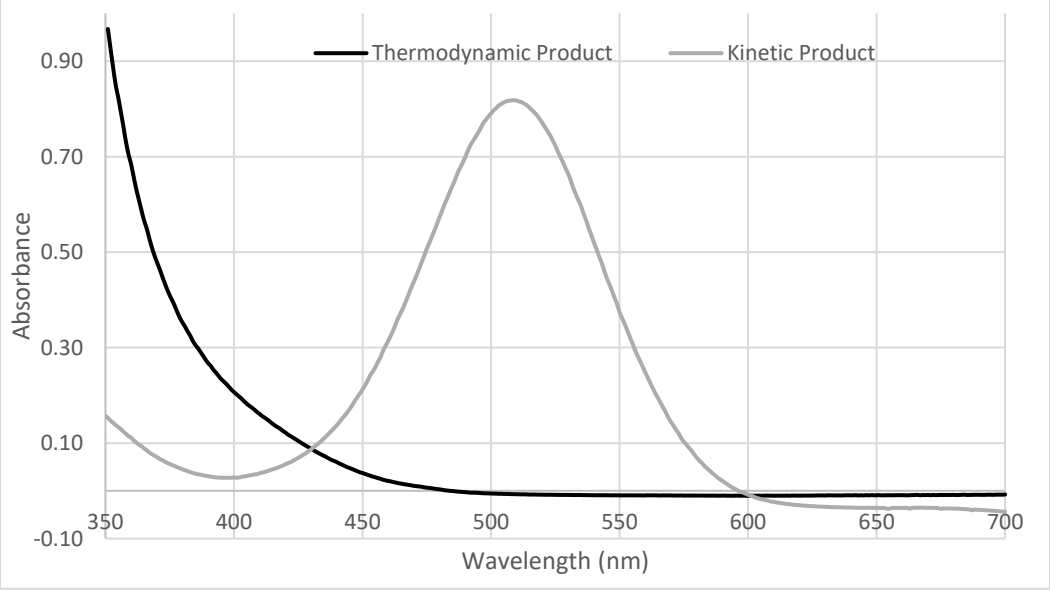

Figure 8. Kinetic and thermodynamic UV Vis absorption shifts of C-propyl pyrogallol[4]arene.

absorbance shifts. Supramolecular self-assembly is assumed to be responsible for the color shifts, with a kinetic supramolecular self-assembly and a thermodynamic self-assembly (Fig. 8). Nearly all pyrogallol[4]arene solutions follow this thermodynamic solution-phase pathway, with a thermodynamically-driven λ_{max} that is shorter than the initial kinetic λ_{max}. The rates and intensities of these shifts vary from solution to solution. Further work is needed to tease out these solution structures and how absorbance correlates with supramolecular self-assembly.

Finally, one last thing to note is that pyrogallol, and to an extent resorcin[4]arenes, exhibit solvatochromism. Teasing out pyrogallol solvatochromism may be helpful to understand pyrogallarane solvatochromism, as pyrogallarenes are merely pyrogallol subunits linked together. Doing this may help deduce which solvatochromic events are properties of isolated hydroxyl rims (pyrogallol) and which solvatochromic events can be attributed to the pyrogallarene macrocycle. Figure 6 shows color changes exhibited when pyrogallol is dissolved in a variety of solvents.

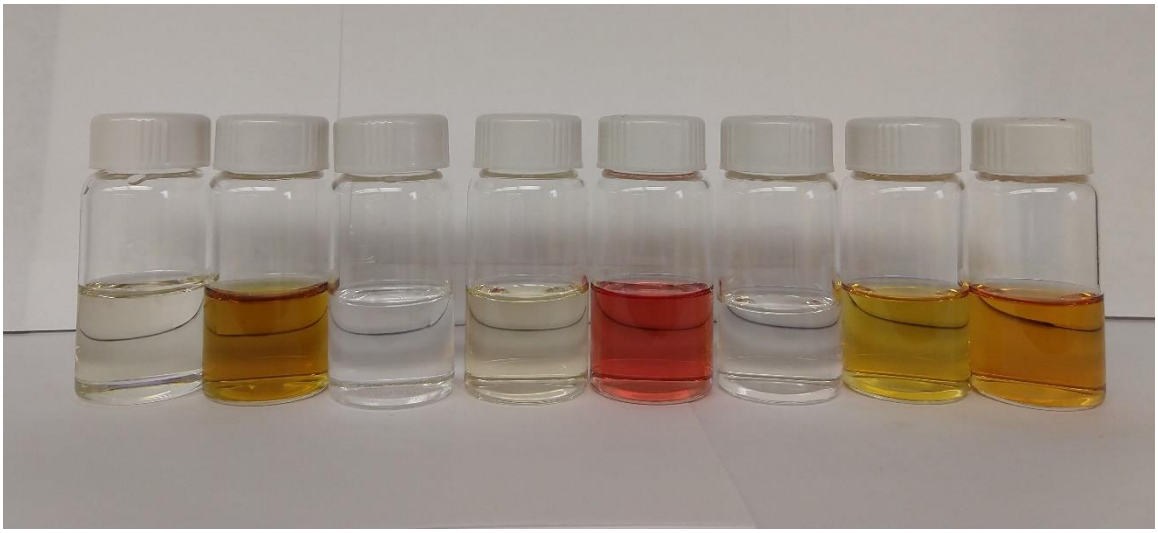

Figure 9. Pyrogallol solutions (originally clear) observed two weeks after 10 mg were added to various organic solvents. Left to right: DMSO, water, $CHCl_3$ (undissolved), 2-propanol, 1,4-dioxane, acetone, methanol, and ethanol.

One major distinction between pyrogallarenes and pyrogallol is that pyrogallol does not exhibit an abrupt absorption shift when titrated over the entire pH range. Instead pyrogallol gradually increases in absorbance from a low pH to a high pH. Historically pyrogallol has been used in a basic solution as a component of the Orsat apparatus to measure atmospheric O_2 or O_2 evolution in reactions.[44,45] Abrash[46] proposed a mechanism for the autoxidation of a similar molecule, di-t-butylpyrogallol, and concluded that the major oxidation product was 3,5-di(2-phenyl-2-propyl)2pyrone-6-carboxylic acid. However, after taking NMR's of pyrogallol one hour after being dissolved in D_2O (colorless) and one month after being dissolved in D_2O (colored) (see Appendix) it is evident that pyrogallol is unchanged throughout these color shifts. The only difference in the NMR spectra is the occurrence of second-order effects in the month-old sample. Whether pyrogallol autoxidation directly correlates with color shifts and whether pyrogallarenes autoxidize to an extent is yet to be determined. It is evident that pyrogallol autoxidation has been reported in biochemical studies,[47–51] but the

mechanism of pyrogallol oxidation has not been thoroughly studied using modern analytical techniques.

CONCLUSION

Pyrogallarenes have the ability to produce a variety of unique structures, including the cocrystal reported herein. One uninteresting pyrogallol[4]arene crystal, *C*-propyl pyrogallol[4]arene·3acetone·$3H_2O$, has been shown to possess unexpected and interesting properties. Vacuum drying of crystal 1 resulted in a quenching of crystal 1's chromophore, and PXRD demonstrated that solvent molecules were removed upon vacuum drying, a hallmark of solvatochromism. Titration of crystal 1 over the entire pH range resulted in the conclusion that *C*-propyl pyrogallol[4]arene is a pH indicator. Exploring pyrogallol[4]arenes with varying tail lengths demonstrated that pH indication is an inherent property of all pyrogallol[4]arenes. Mapping of hydrogen bonding interactions in crystal 1 revealed that water acts primarily as a base in crystal 1, yet the hydroxyl rim of crystal 1 is protonated. Crystal 2 corroborates solvatochromism found in crystal 1, despite having a greater degree of disorder. Ultimately, the anamorphic changes of pyrogallarene absorbance over time without pyrogallarene degradation suggest that self-assembly may be traced through solvatochromic interactions. Pyrogallarene solvatochromism is an area that has been previously overlooked but holds great potential to expand understanding of supramolecular structures and self-assembly.

BIBLIOGRAPHY

(1) MacGillivray, L. R.; Atwood, J. L. A Chiral Spherical Molecular Assembly Held Together by 60 Hydrogen Bonds. *Nature* **1997**, *389*, 469–472.

(2) Gerkensmeier, T.; Iwanek, W.; Agena, C.; Fröhlich, R.; Kotila, S.; Näther, C.; Mattay, J. Self-Assembly of 2,8,14,20-Tetraisobutyl-5,11,17,23-Tetrahydroxyresorc[4]Arene. *Eur. J. Org. Chem.* **1999**, *1999* (9), 2257–2262.

(3) Zhang, C.; Patil, R. S.; Liu, C.; Barnes, C. L.; Atwood, J. L. Controlled 2D Assembly of Nickel-Seamed Hexameric Pyrogallol[4]Arene Nanocapsules. *Journal of the American Chemical Society* **2017**, *139* (8), 2920–2923.

(4) Zhang, C.; Patil, R. S.; Li, T.; Barnes, C. L.; Atwood, J. L. Self-Assembly of Magnesium-Seamed Hexameric Pyrogallol[4]Arene Nanocapsules. *Chemical Communications* **2017**, *53* (31), 4312–4314.

(5) Rathnayake, A. S.; Barnes, C. L.; Atwood, J. L. Zinc(II)-Directed Self-Assembly of Metal–Organic Nanocapsules. *Crystal Growth & Design* **2017**, *17* (9), 4501–4503.

(6) Rathnayake, A. S.; Feaster, K. A.; White, J.; Barnes, C. L.; Teat, S. J.; Atwood, J. L. Investigating Reaction Conditions To Control the Self-Assembly of Cobalt-Seamed Nanocapsules. *Crystal Growth & Design* **2016**, *16* (7), 3562–3564.

(7) Kumari, H.; Kline, S. R.; Schuster, N. J.; Atwood, J. L. Solution Structure of Copper-Seamed C-Alkylpyrogallol[4]Arene Nanocapsules with Varying Chain Lengths. *Chemical Communications* **2011**, *47* (45), 12298.

(8) Kumari, H.; Jin, P.; Teat, S. J.; Barnes, C. L.; Dalgarno, S. J.; Atwood, J. L. Strong Cation···π Interactions Promote the Capture of Metal Ions within Metal-Seamed Nanocapsule. *Journal of the American Chemical Society* **2014**, *136* (49), 17002–17005.

(9) Danylyuk, O.; Suwinska, K. Solid-State Interactions of Calixarenes with Biorelevant Molecules. *Chemical Communications* **2009**, No. 39, 5799.

(10) Wenger, M.; Bernstein, J. An Alternate Crystal Form of Gabapentin: A Cocrystal with Oxalic Acid. *Crystal Growth & Design* **2008**, *8* (5), 1595–1598.

(11) André, V.; Marques, M. M.; da Piedade, M. F. M.; Duarte, M. T. An Ester Derivative of the Drug Gabapentin: PH Dependent Crystal Stability. *Journal of Molecular Structure* **2010**, *973* (1–3), 173–179.

(12) Reddy, L. S.; Bethune, S. J.; Kampf, J. W.; Rodríguez-Hornedo, N. Cocrystals and Salts of Gabapentin: PH Dependent Cocrystal Stability and Solubility. *Crystal Growth & Design* **2009**, *9* (1), 378–385.

(13) Wenger, M.; Bernstein, J. Designing a Cocrystal of γ-Amino Butyric Acid. *Angewandte Chemie International Edition* **2006**, *45* (47), 7966–7969.

(14) Agarwal, P.; Griffith, A.; Costantino, H. R.; Vaish, N. Gabapentin Enacarbil - Clinical Efficacy in Restless Legs Syndrome. *Neuropsychiatr. Dis. Treat.* **2010**, *2010* (6), 151–158.

(15) Rodríguez-Spong, B. General Principles of Pharmaceutical Solid Polymorphism A Supramolecular Perspective. *Advanced Drug Delivery Reviews* **2004**, *56* (3), 241–274.

(16) Fowler, D. A.; Tian, J.; Barnes, C.; Teat, S. J.; Atwood, J. L. Cocrystallization of C-Butyl Pyrogallol[4]Arene and C-Propan-3-Ol Pyrogallol[4]Arene with Gabapentin. *CrystEngComm* **2011**, *13* (5), 1446–1449.
(17) Cremer, P. S.; Flood, A. H.; Gibb, B. C.; Mobley, D. L. Collaborative Routes to Clarifying the Murky Waters of Aqueous Supramolecular Chemistry. *Nature Chemistry* **2017**, *10* (1), 8–16.
(18) Dalgarno, S. J.; Bassil, D. B.; Tucker, S. A.; Atwood, J. L. Cocrystallization and Encapsulation of a Fluorophore with Hexameric Pyrogallol[4]Arene Nanocapsules: Structural and Fluorescence Studies. *Angewandte Chemie International Edition* **2006**, *45* (42), 7019–7022.
(19) Pfeiffer, C. R.; Fowler, D. A.; Atwood, J. L. Establishing Trends Based on Solvent System Changes in Cocrystals Containing Pyrogallol[4]Arenes and Fluorescent Probes Rhodamine B and Pyronin Y. *CrystEngComm* **2015**, *17* (24), 4475–4485.
(20) Chandrasekaran, S.; Enoch, I. V. M. V. Host–guest Interaction of Flavanone and 7-Aminoflavone with C-Hexylpyrogallol[4]Arene. *Journal of Molecular Structure* **2014**, *1076*, 318–325.
(21) Pfeiffer, C. R.; Atwood, S. G.; Samadello, L.; Atwood, J. L. Investigating Properties and Trends of Cocrystals Composed of Pyrogallol[4]Arenes and Anthracene-Based Fluorescent Probes. *Crystal Growth & Design* **2015**, *15* (6), 2958–2978.
(22) Kim, J.-K.; Lee, H. A.; Lee, H.; Chung, H. J. Phenolic Pyrogallol Fluorogen for Red Fluorescence Development in a PAS Domain Protein. *Chemistry of Materials* **2018**, *30* (5), 1467–1471.
(23) Pfeiffer, C. R.; Fowler, D. A.; Atwood, J. L. Selective Complexation in Three Component Cocrystals Composed of Pyrogallol[4]Arene and Fluorescent Probes Pyrene and 1-(2-Pyridylazo)-2-Naphthol. *Crystal Growth & Design* **2015**, *15* (8), 3992–3998.
(24) Bassil, D. B.; Dalgarno, S. J.; Cave, G. W. V.; Atwood, J. L.; Tucker, S. A. Spectroscopic Investigations of ADMA Encapsulated in Pyrogallol[4]Arene Nanocapsules. *The Journal of Physical Chemistry B* **2007**, *111* (30), 9088–9092.
(25) Whetstine, J. L.; Kline, K. K.; Fowler, D. A.; Ragan, C. M.; Barnes, C. L.; Atwood, J. L.; Tucker, S. A. Spectroscopic Investigations of Pyrene Butanol Encapsulated in C-Hexylpyrogallol[4]Arene Nanocapsules. *New Journal of Chemistry* **2010**, *34* (11), 2587.
(26) Barrett, E. S.; Dale, T. J.; Rebek, J. Synthesis and Assembly of Monofunctionalized Pyrogallolarene Capsules Monitored by Fluorescence Resonance Energy Transfer. *Chemical Communications* **2007**, No. 41, 4224.
(27) Barrett, E. S.; Dale, T. J.; Rebek, J. Stability, Dynamics, and Selectivity in the Assembly of Hydrogen-Bonded Hexameric Capsules. *Journal of the American Chemical Society* **2008**, *130* (7), 2344–2350.
(28) Reichardt, C. Solvents and Solvent Effects: An Introduction. *Organic Process Research & Development* **2007**, *11* (1), 105–113.
(29) Reichardt, C. Solvatochromic Dyes as Solvent Polarity Indicators. *Chemical Reviews* **1994**, *94* (8), 2319–2358.

(30) Marini, A.; Muñoz-Losa, A.; Biancardi, A.; Mennucci, B. What Is Solvatochromism? *The Journal of Physical Chemistry B* **2010**, *114* (51), 17128–17135.
(31) Kumari, H.; Deakyne, C. A.; Atwood, J. L. Solution Structures of Nanoassemblies Based on Pyrogallol[4]Arenes. *Accounts of Chemical Research* **2014**, *47* (10), 3080–3088.
(32) Funck, M.; Guest, D. P.; Cave, G. W. V. Microwave-Assisted Synthesis of Resorcin[4]Arene and Pyrogallol[4]Arene Macrocycles. *Tetrahedron Letters* **2010**, *51* (49), 6399–6402.
(33) Dalgarno, S. J.; Power, N. P.; Atwood, J. L. Metallo-Supramolecular Capsules. *Coordination Chemistry Reviews* **2008**, *252* (8–9), 825–841.
(34) Spek, A. L. It PLATON SQUEEZE: A Tool for the Calculation of the Disordered Solvent Contribution to the Calculated Structure Factors. *Acta Crystallographica Section C* **2015**, *71* (1), 9–18.
(35) Sheldrick, G. M. Crystal Structure Refinement with *SHELXL*. *Acta Crystallographica Section C Structural Chemistry* **2015**, *71* (1), 3–8.
(36) Dolomanov, O. V.; Bourhis, L. J.; Gildea, R. J.; Howard, J. A. K.; Puschmann, H. *OLEX2* : A Complete Structure Solution, Refinement and Analysis Program. *Journal of Applied Crystallography* **2009**, *42* (2), 339–341.
(37) Macrae, C. F.; Bruno, I. J.; Chisholm, J. A.; Edgington, P. R.; McCabe, P.; Pidcock, E.; Rodriguez-Monge, L.; Taylor, R.; van de Streek, J.; Wood, P. A. *Mercury CSD 2.0* – New Features for the Visualization and Investigation of Crystal Structures. *Journal of Applied Crystallography* **2008**, *41* (2), 466–470.
(38) Torshin, I. Y.; Weber, I. T.; Harrison, R. W. Geometric Criteria of Hydrogen Bonds in Proteins and Identification of `bifurcated' Hydrogen Bonds. *Protein Engineering, Design and Selection* **2002**, *15* (5), 359–363.
(39) *The Weak Hydrogen Bond: In Structural Chemistry and Biology*; International Union of Crystallography Monographs on Crystallography; Oxford University Press: Oxford, New York, 2001.
(40) McDonald, I. K.; Thornton, J. M. Satisfying Hydrogen Bond Potential in Proteins. *Journal of Molecular Biology* **1994**, *238* (5), 777–793.
(41) Kumari, H.; Zhang, J.; Erra, L.; Barbour, L. J.; Deakyne, C. A.; Atwood, J. L. Cocrystals of Gabapentin with C-Alkylresorcin[4]Arenes. *CrystEngComm* **2013**, *15* (20), 4045.
(42) Atwood, J. L.; Barbour, L. J.; Jerga, A. On the Synthesis and Structure of the Very Large Spherical Capsules Derived from Hexamers of Pyrogallol[4]Arenes. *Journal of Supramolecular Chemistry* **2001**, *1* (3), 131–134.
(43) Wang, Q.; Li, R.; Qiu, S.; Lin, Z.; Chen, G.; Luo, L. A Colorimetric Sensor for PH Utilizing a Quinoline Derivative. *Analytical Methods* **2014**, *6* (14), 5016.
(44) Forster, A. C. A Rapid Determination of Oxygen in the Air. *Journal of Chemical Education* **1927**, *4* (5), 638.
(45) Fieldner, A. C.; Jones, G. W.; Holbrook, W. F. The Bureau of Mines Orsat Apparatus for Gas Analysis. **1925**, No. Technical Paper 320, 1.
(46) Abrash, H. I. The Air Oxidation of 4,6-Di (2-Phenyl-2-Propyl) Pyrogallol. Spectroscopic and Kinetic Studies of the Intermediates. *Carlsberg Research Communications* **1977**, *42* (1), 11–25.

(47) Marklund, S.; Marklund, G. Involvement of the Superoxide Anion Radical in the Autoxidation of Pyrogallol and a Convenient Assay for Superoxide Dismutase. *European Journal of Biochemistry* **1974**, *47* (3), 469–474.
(48) Gaikwad, K. K.; Lee, Y. S. Novel Natural Phenolic Compound-Based Oxygen Scavenging System for Active Packaging Applications. *Journal of Food Measurement and Characterization* **2016**, *10* (3), 533–538.
(49) Mu, S.; Chen, C. Electrochemical Oxidation of Pyrogallol: Formation and Characterization of Long-Lived Oxygen Radicals and Application To Assess the Radical Scavenging Abilities of Antioxidants. *The Journal of Physical Chemistry B* **2012**, *116* (41), 12567–12573.
(50) Gao, R.; Yuan, Z.; Zhao, Z.; Gao, X. Mechanism of Pyrogallol Autoxidation and Determination of Superoxide Dismutase Enzyme Activity. *Bioelectrochemistry and Bioenergetics* **1998**, *45* (1), 41–45.
(51) Ramasarma, T.; Rao, A. V. S.; Devi, M. M.; Omkumar, R. V.; Bhagyashree, K. S.; Bhat, S. V. New Insights of Superoxide Dismutase Inhibition of Pyrogallol Autoxidation. *Molecular and Cellular Biochemistry* **2015**, *400* (1–2), 277–285.
(52) Nikolayenko, V. I.; van Wyk, L. M.; Munro, O. Q.; Barbour, L. J. Supramolecular Solvatochromism: Mechanistic Insight from Crystallography, Spectroscopy and Theory. *Chemical Communications* **2018**, *54* (51), 6975–6978.

APPENDIX

Thermal ellipsoid of cocrystal 1

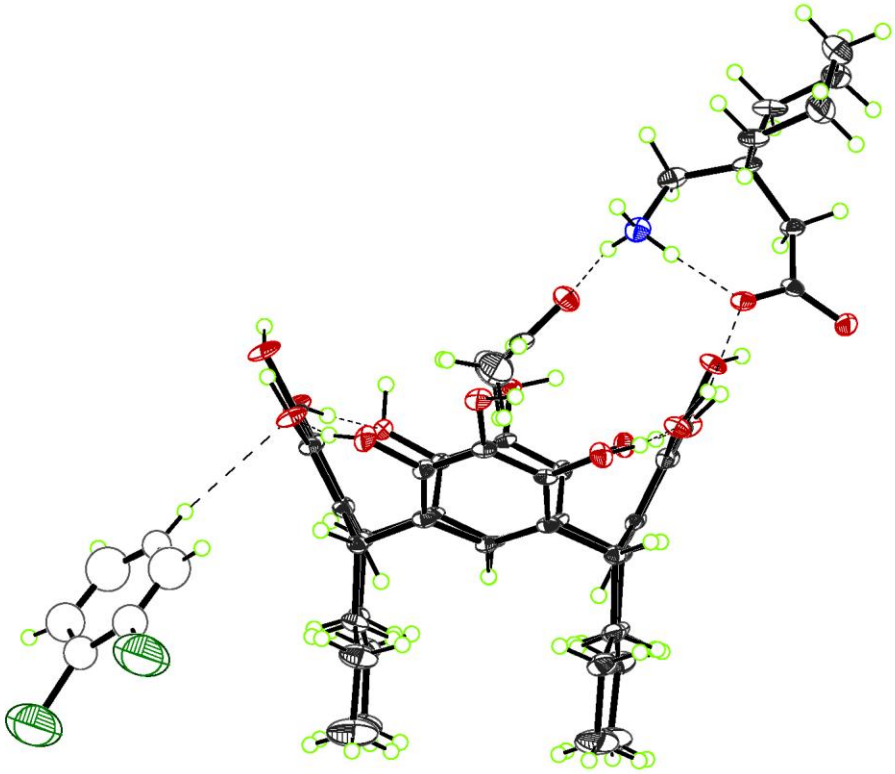

Thermal ellipsoid of cocrystal 1

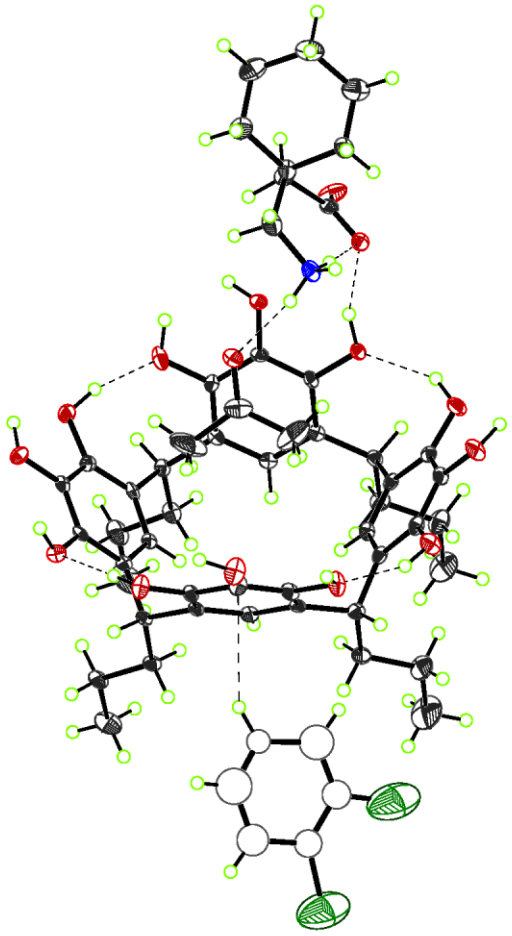

CheckCIF of Cocrystal 1

checkCIF/PLATON report

Structure factors have been supplied for datablock(s) sl_sq

THIS REPORT IS FOR GUIDANCE ONLY. IF USED AS PART OF A REVIEW PROCEDURE FOR PUBLICATION, IT SHOULD NOT REPLACE THE EXPERTISE OF AN EXPERIENCED CRYSTALLOGRAPHIC REFEREE.

No syntax errors found. CIF dictionary Interpreting this report

Datablock: sl_sq

Bond precision: C-C = 0.0061 A Wavelength=0.71073

Cell: a=11.7633(9) b=15.6968(12) c=17.8554(14)
alpha=71.988(2) beta=82.735(3) gamma=71.812(3)
Temperature: 100 K

	Calculated	Reported
Volume	2977.1(4)	2977.1(4)
Space group	P -1	P -1
Hall group	-P 1	-P 1
Moiety formula	C40 H48 O12, 0.5(C6 H4 C12), C9 H17 N O2, C3 H6 O [+ solvent]	C40 H48 O12, C9 H17 N O2, C3 H6 O, C3 H2 Cl
Sum formula	C55 H73 Cl N O15 [+ solvent]	C55 H73 Cl N O15
Mr	1023.59	1023.59
Dx,g cm-3	1.142	1.142
Z	2	2
Mu (mm-1)	0.125	0.125
F000	1094.0	1094.0
F000'	1094.87	
h,k,lmax	14,19,22	14,19,22
Nref	12542	12406
Tmin,Tmax	0.982,0.990	0.636,0.745
Tmin'	0.957	

Correction method= # Reported T Limits: Tmin=0.636 Tmax=0.745
AbsCorr = MULTI-SCAN

Data completeness= 0.989 Theta(max)= 26.655

R(reflections)= 0.0965(7684) wR2(reflections)= 0.2686(12406)

S = 1.044 Npar= 691

CheckCIF of Crystal 1 (*C*-propyl pyrogallol[4]arene·3acetone·3H_2O)

checkCIF/PLATON report

Structure factors have been supplied for datablock(s) s1

THIS REPORT IS FOR GUIDANCE ONLY. IF USED AS PART OF A REVIEW PROCEDURE FOR PUBLICATION, IT SHOULD NOT REPLACE THE EXPERTISE OF AN EXPERIENCED CRYSTALLOGRAPHIC REFEREE.

No syntax errors found. CIF dictionary Interpreting this report

Datablock: s1

Bond precision: C-C = 0.0022 A Wavelength=1.54178

Cell: a=11.6328(3) b=12.8379(4) c=17.5278(5)
alpha=104.0573(15) beta=95.6629(15) gamma=101.6170(16)
Temperature: 100 K

	Calculated	Reported
Volume	2457.03(12)	2457.02(12)
Space group	P -1	P -1
Hall group	-P 1	-P 1
Moiety formula	C40 H48 O12, 3(C3 H6 O), 3(H2 O)	C40 H48 O12, 3(C3 H6 O), 3(H2 O)
Sum formula	C49 H72 O18	C49 H72 O18
Mr	949.07	949.06
Dx,g cm-3	1.283	1.283
Z	2	2
Mu (mm-1)	0.808	0.808
F000	1020.0	1020.0
F000'	1023.44	
h,k,lmax	14,16,21	13,15,21
Nref	9975	9641
Tmin,Tmax	0.899,0.937	0.661,0.754
Tmin'	0.778	

Correction method= # Reported T Limits: Tmin=0.661 Tmax=0.754
AbsCorr = MULTI-SCAN

Data completeness= 0.967 Theta(max)= 74.014

R(reflections)= 0.0414(8062) wR2(reflections)= 0.1076(9641)

S = 1.022 Npar= 640

CheckCIF of Crystal 2 (*C*-ethyl pyrogallol[4]arene·acetone·nH_2O)

checkCIF/PLATON report

Structure factors have been supplied for datablock(s) sl_sq

THIS REPORT IS FOR GUIDANCE ONLY. IF USED AS PART OF A REVIEW PROCEDURE FOR PUBLICATION, IT SHOULD NOT REPLACE THE EXPERTISE OF AN EXPERIENCED CRYSTALLOGRAPHIC REFEREE.

No syntax errors found. CIF dictionary Interpreting this report

Datablock: sl_sq

Bond precision: C-C = 0.0043 A Wavelength=0.71073

Cell: a=11.6986(9) b=12.3868(9) c=16.8118(12)
alpha=83.621(3) beta=78.348(3) gamma=75.848(3)
Temperature: 273 K

	Calculated	Reported
Volume	2308.7(3)	2308.7(3)
Space group	P -1	P -1
Hall group	-P 1	-P 1
Moiety formula	2(C36 H40 O12), 2(C3 H6 O), 7(O), 4(H2 O) [+ solvent]	C36 H40 O12, 3.5(O), 2(H2 O), C3 H6 O
Sum formula	C78 H100 O37 [+ solvent]	C39 H50 O18.50
Mr	1629.58	814.79
Dx,g cm-3	1.172	1.172
Z	1	2
Mu (mm-1)	0.094	0.094
F000	864.0	864.0
F000'	864.56	
h,k,lmax	15,16,21	15,16,21
Nref	10705	10637
Tmin,Tmax	0.993,0.996	0.654,0.746
Tmin'	0.980	

Correction method= # Reported T Limits: Tmin=0.654 Tmax=0.746
AbsCorr = MULTI-SCAN

Data completeness= 0.994 Theta(max)= 27.597

R(reflections)= 0.0793(7120) wR2(reflections)= 0.2403(10637)

S = 1.027 Npar= 535

(all NMR's embedded as PDF's within the document)

NMRs of PgC_3 three hours after being dissolved in 90/10 v/v Acetone/D_2O

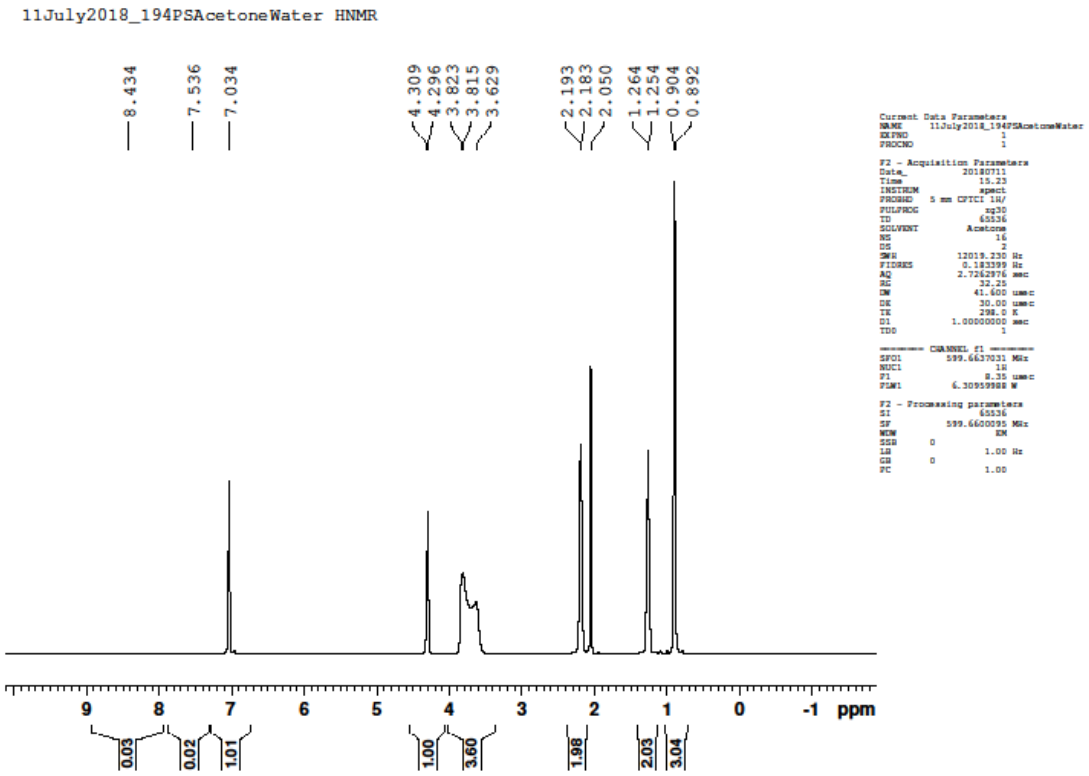

11July2018_194PSAcetoneWater HNMR

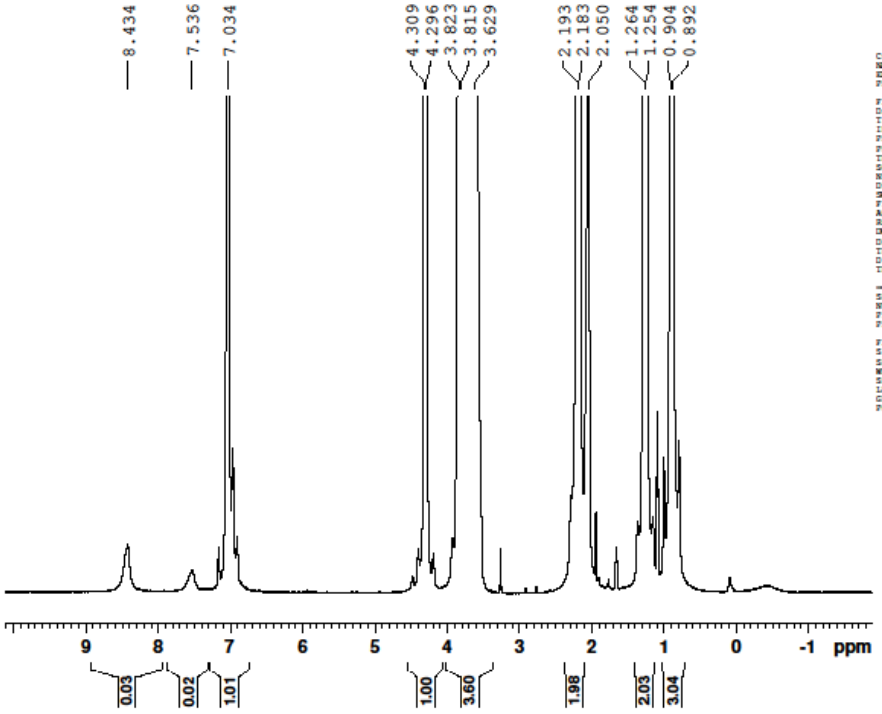


```
Current Data Parameters
NAME      11July2018_194PSAcetoneWater
EXPNO                 1
PROCNO                1

F2 - Acquisition Parameters
Date_           20180711
Time              15.23
INSTRUM             spect
PROBHD   5 mm CPTCI 1H/
PULPROG             zg30
TD                 65536
SOLVENT          Acetone
NS                    16
DS                     2
SWH            12019.230 Hz
FIDRES          0.183399 Hz
AQ              2.7262976 sec
RG                 32.25
DW                41.600 usec
DE                30.00 usec
TE                298.0 K
D1             1.00000000 sec
TD0                    1

======== CHANNEL f1 ========
SFO1          599.6637031 MHz
NUC1                  1H
P1                 8.35 usec
PLW1          6.30959988 W

F2 - Processing parameters
SI                 65536
SF            599.6600095 MHz
WDW                   EM
SSB                    0
LB                  1.00 Hz
GB                     0
PC                  1.00
```

11July2018_194PSAcetoneWater CNMR

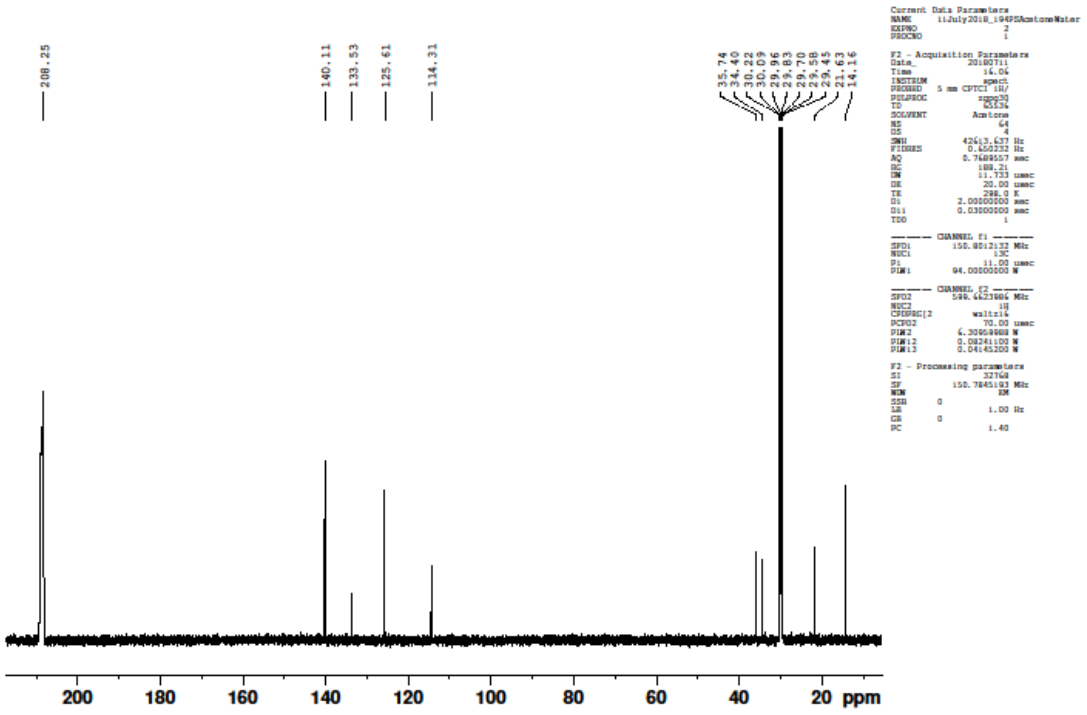

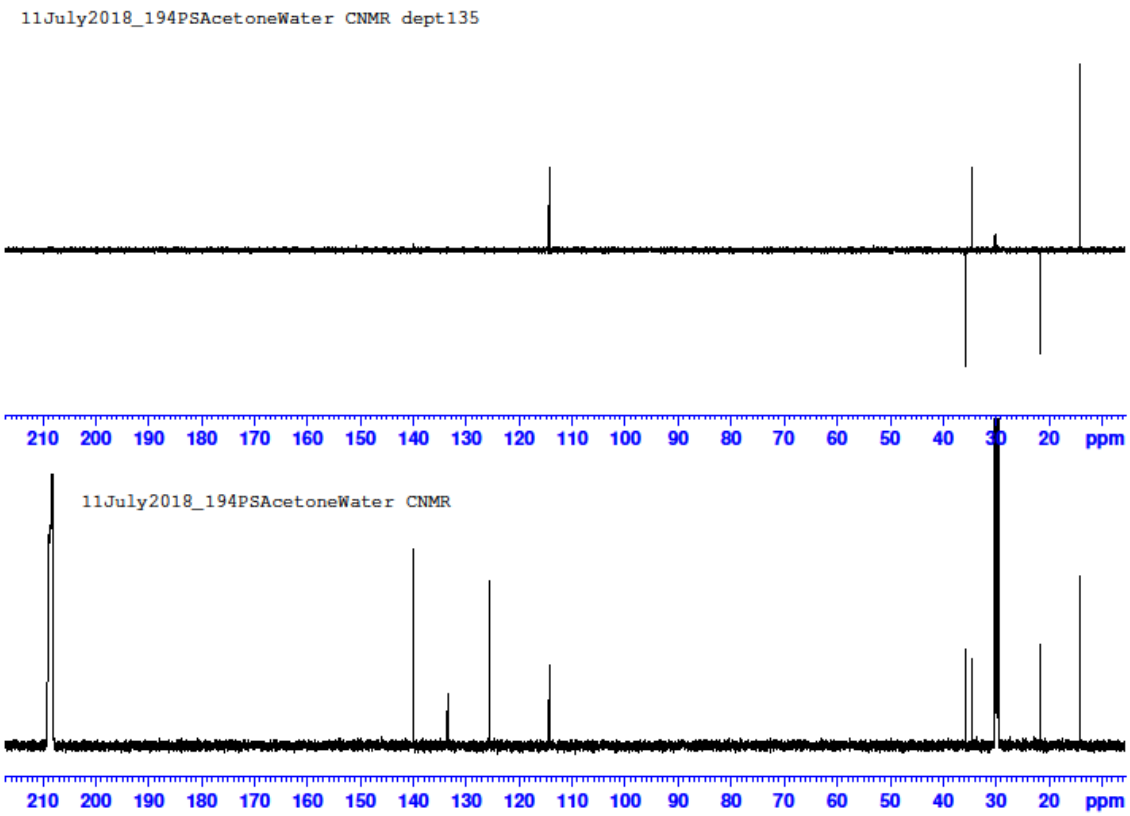
11July2018_194PSAcetoneWater CNMR dept135
210 200 190 180 170 160 150 140 130 120 110 100 90 80 70 60 50 40 30 20 ppm
11July2018_194PSAcetoneWater CNMR
210 200 190 180 170 160 150 140 130 120 110 100 90 80 70 60 50 40 30 20 ppm

NMRs of PgC_3 five days after being dissolved in 90/10 v/v Acetone/D_2O

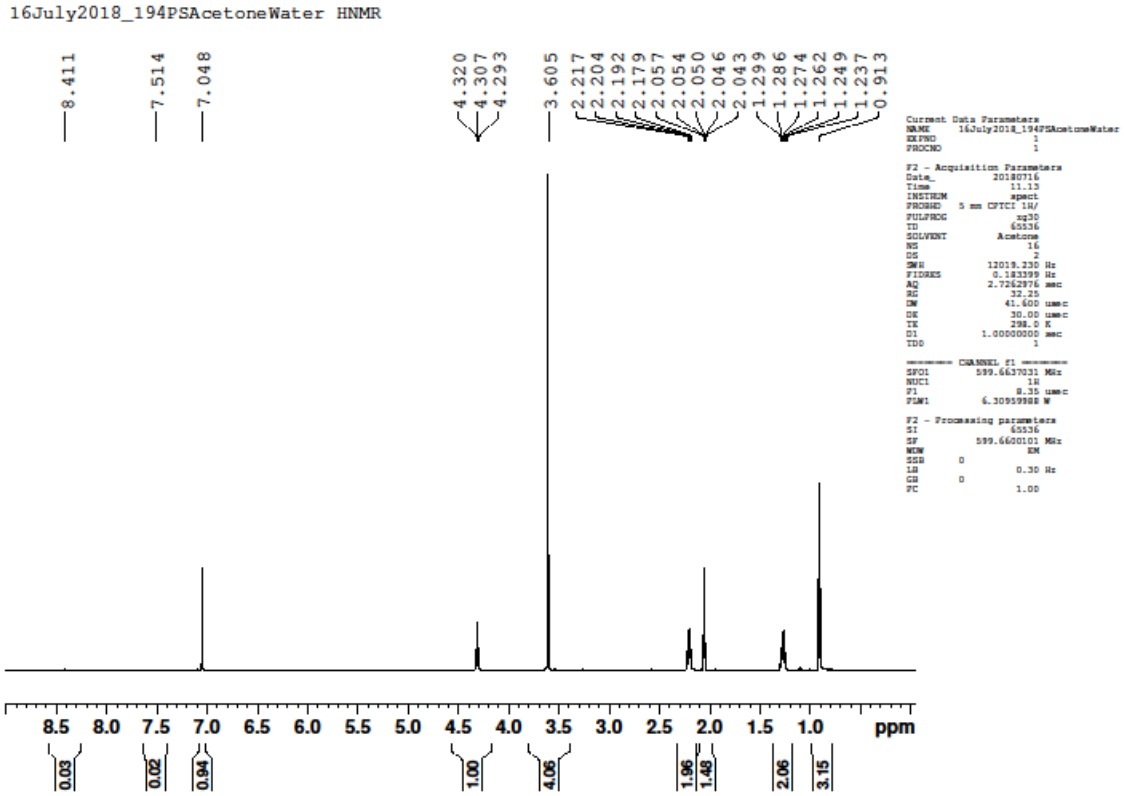

16July2018_194PSAcetoneWater HNMR

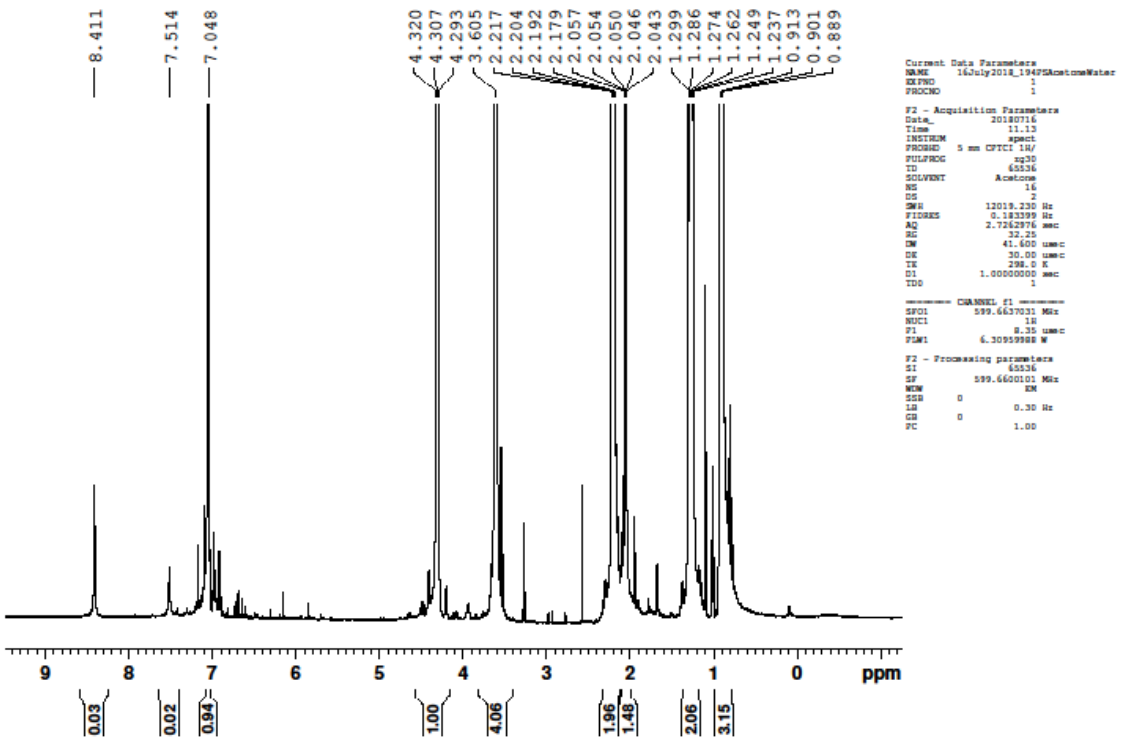

Current Data Parameters
NAME 16July2018_194PSAcetoneWater
EXPNO 1
PROCNO 1

F2 - Acquisition Parameters
Date_ 20180716
Time 11.13
INSTRUM spect
PROBHD 5 mm CPTCI 1H/
PULPROG zg30
TD 65536
SOLVENT Acetone
NS 16
DS 2
SWH 12019.230 Hz
FIDRES 0.183399 Hz
AQ 2.7262976 sec
RG 32.25
DW 41.600 usec
DE 30.00 usec
TE 298.0 K
D1 1.00000000 sec
TD0 1

======== CHANNEL f1 ========
SFO1 599.6637031 MHz
NUC1 1H
P1 8.35 usec
PLW1 6.30959988 W

F2 - Processing parameters
SI 65536
SF 599.6600101 MHz
WDW EM
SSB 0
LB 0.30 Hz
GB 0
PC 1.00

16July2018_194PSAcetoneWater HNMR

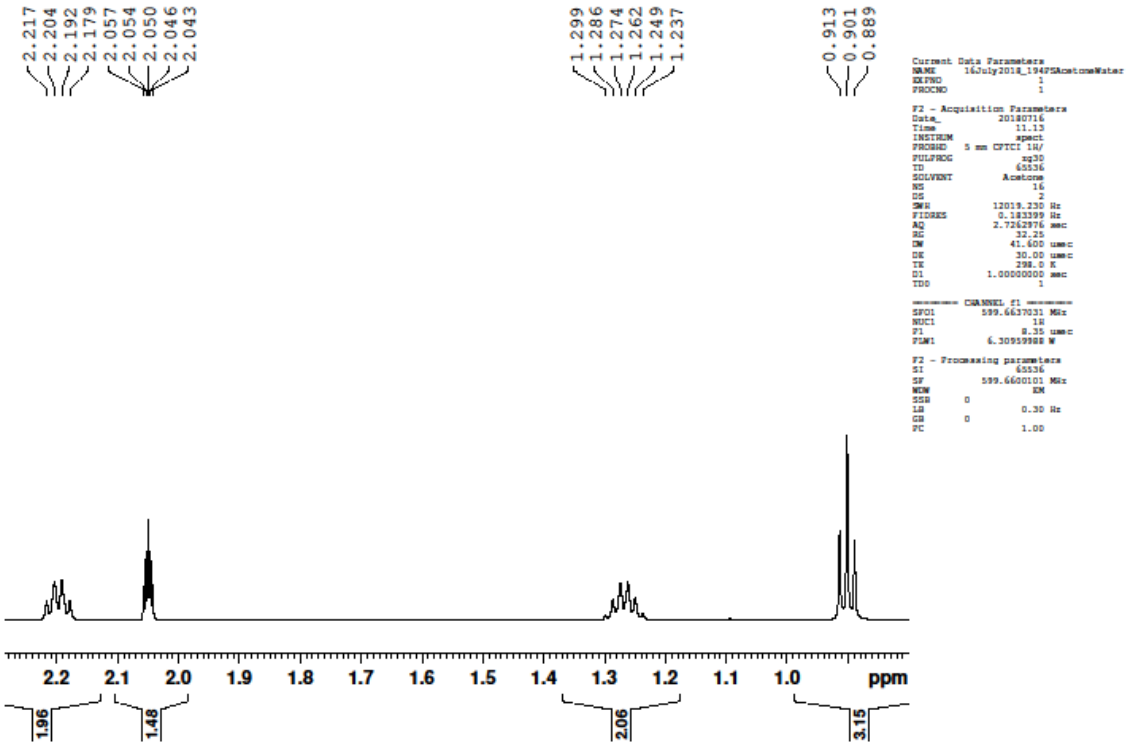


```
Current Data Parameters
NAME      16July2018_194PSAcetoneWater
EXPNO                 1
PROCNO                1

F2 - Acquisition Parameters
Date_          20180716
Time              11.13
INSTRUM             spect
PROBHD   5 mm CPTCI 1H/
PULPROG             zg30
TD                 65536
SOLVENT          Acetone
NS                    16
DS                     2
SWH            12019.230 Hz
FIDRES             0.183399 Hz
AQ             2.7262976 sec
RG                 32.25
DW                41.600 usec
DE                30.00 usec
TE                298.0 K
D1             1.00000000 sec
TD0                    1

======== CHANNEL f1 ========
SFO1          599.6637031 MHz
NUC1                  1H
P1                 8.35 usec
PLW1           6.30959988 W

F2 - Processing parameters
SI                 65536
SF            599.6600101 MHz
WDW                   EM
SSB       0
LB                 0.30 Hz
GB        0
PC                 1.00
```

16July2018_194PSAcetoneWater HNMR

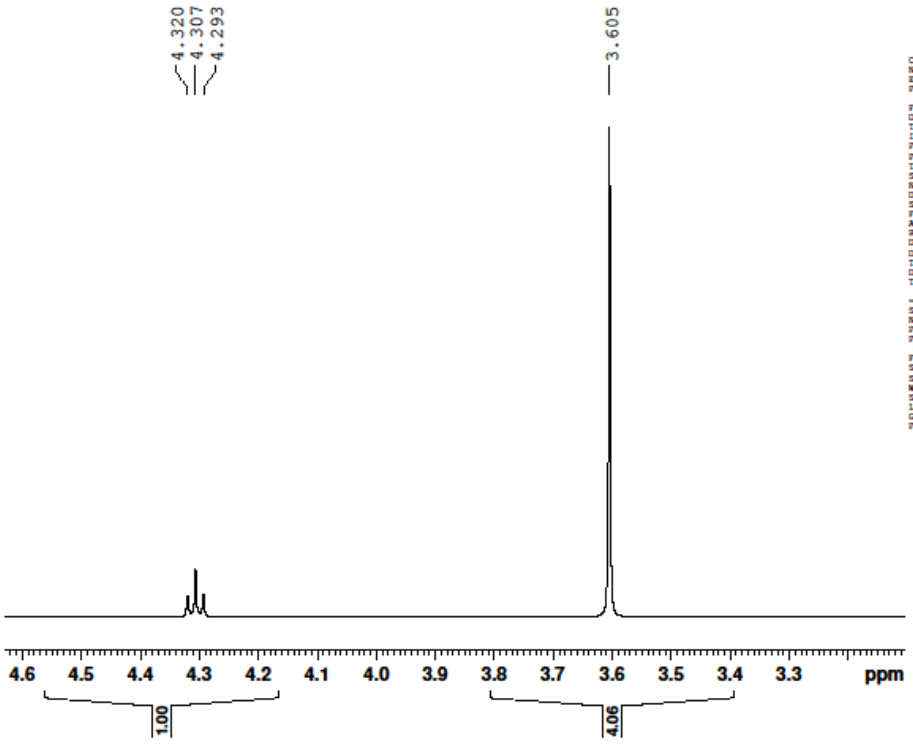


```
Current Data Parameters
NAME      16July2018_194PSAcetoneWater
EXPNO                 1
PROCNO                1

F2 - Acquisition Parameters
Date_          20180716
Time              11.13
INSTRUM           spect
PROBHD  5 mm CPTCI 1H/
PULPROG          zg30
TD              65536
SOLVENT       Acetone
NS                   16
DS                    2
SWH           12019.230 Hz
FIDRES        0.183399 Hz
AQ            2.7262976 sec
RG                32.25
DW               41.600 usec
DE               30.00 usec
TE              298.0 K
D1           1.00000000 sec
TD0                   1

======== CHANNEL f1 ========
SFO1        599.6637031 MHz
NUC1                1H
P1                8.35 usec
PLW1         6.30959988 W

F2 - Processing parameters
SI                65536
SF          599.6600101 MHz
WDW                  EM
SSB       0
LB                0.30 Hz
GB        0
PC                1.00
```

16July2018_194PSAcetoneWater 13CNMR

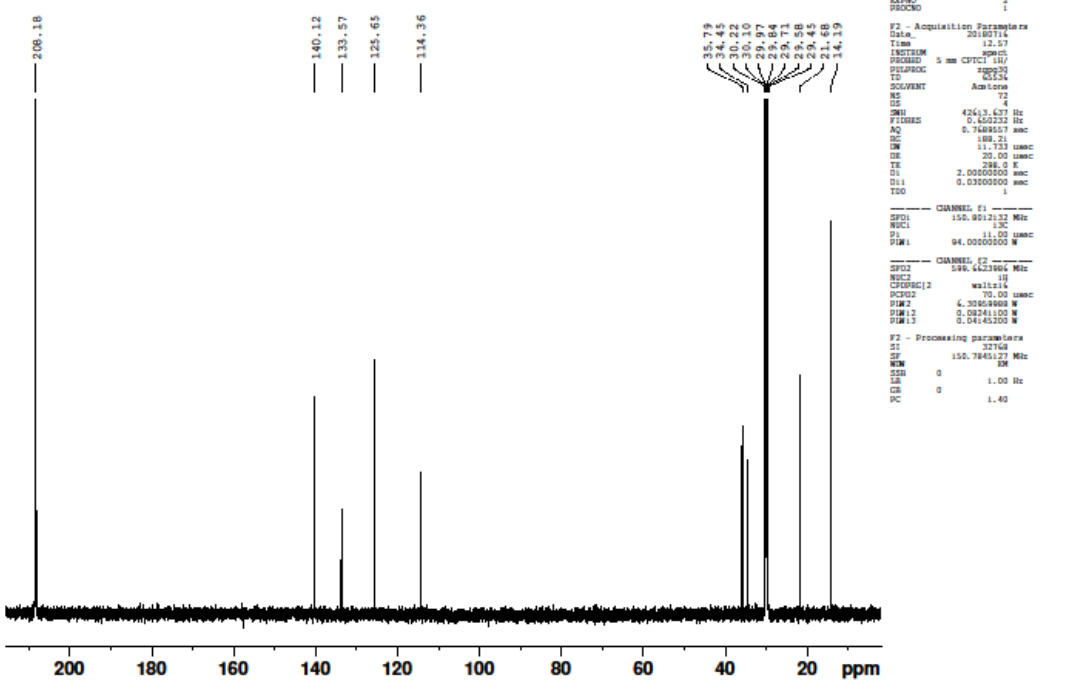

Current Data Parameters
NAME 16July2018_194PSAcetoneWater
EXPNO 2
PROCNO 1

F2 - Acquisition Parameters
Date_ 20180714
Time 12.57
INSTRUM spect
PROBHD 5 mm CPTCI 1H/
PULPROG zgpg30
TD 65536
SOLVENT Acetone
NS 72
DS 4
SWH 42613.627 Hz
FIDRES 0.650232 Hz
AQ 0.7689557 sec
RG 188.21
DW 11.733 usec
DE 20.00 usec
TE 298.0 K
D1 2.00000000 sec
D11 0.03000000 sec
TD0 1

======== CHANNEL f1 ========
SFO1 150.9012132 MHz
NUC1 13C
P1 11.00 usec
PLW1 94.00000000 W

======== CHANNEL f2 ========
SFO2 599.6623804 MHz
NUC2 1H
CPDPRG[2 waltz16
PCPD2 70.00 usec
PLW2 6.30959988 W
PLW12 0.08241100 W
PLW13 0.04165300 W

F2 - Processing parameters
SI 32768
SF 150.7845127 MHz
WDW EM
SSB 0
LB 1.00 Hz
GB 0
PC 1.40

NMRs of PgC_3 three weeks after being dissolved in 90/10 v/v Acetone/D_2O

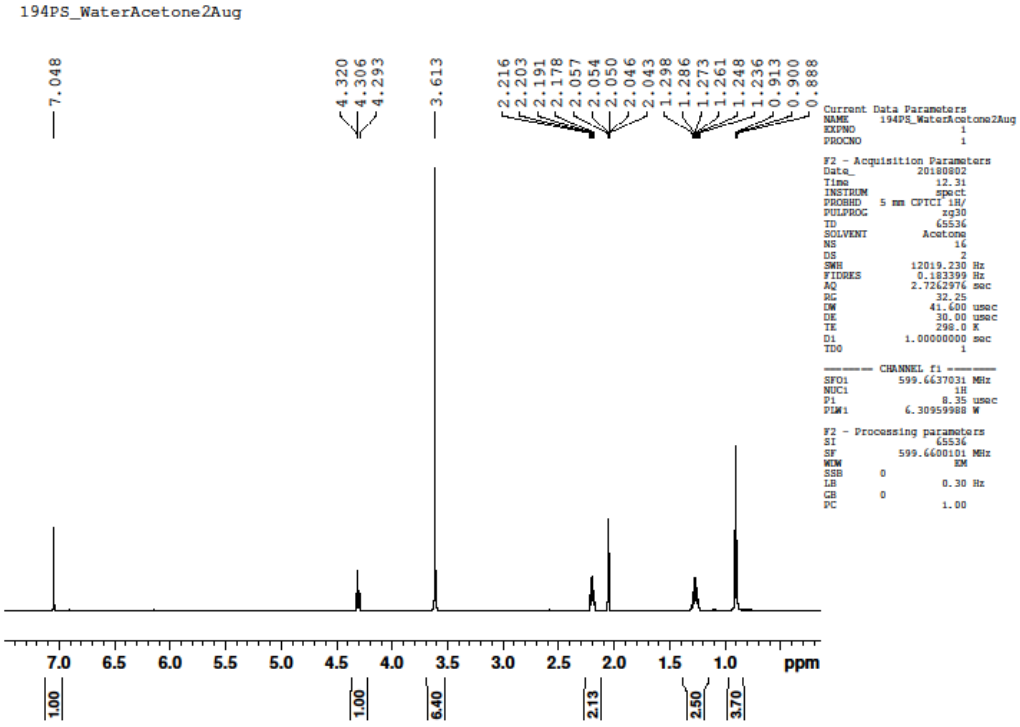

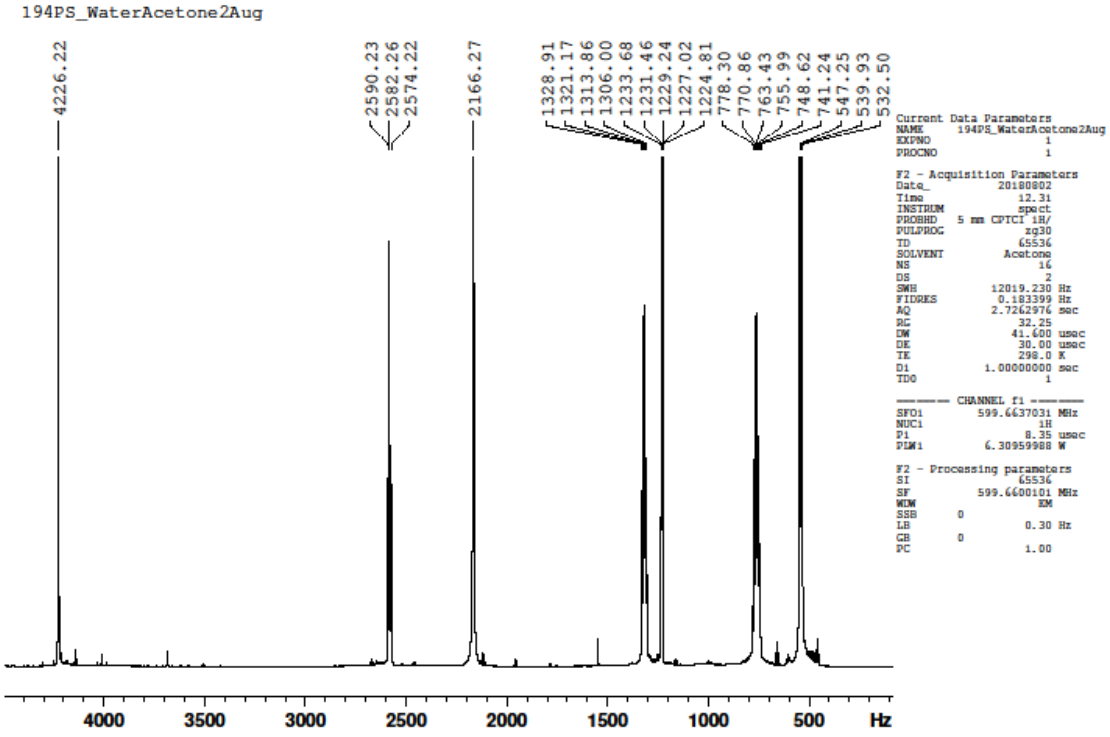
194PS_WaterAcetone2Aug
4226.22
2590.23
2582.26
2574.22
2166.27
1328.91
1321.17
1313.86
1306.00
1233.68
1231.46
1229.24
1227.02
1224.81
778.30
770.86
763.43
755.99
748.62
741.24
547.25
539.93
532.50
4000
3500
3000
2500
2000
1500
1000
500
Hz
Current Data Parameters
NAME 194PS_WaterAcetone2Aug
EXPNO 1
PROCNO 1
F2 - Acquisition Parameters
Date_ 20180802
Time 12.31
INSTRUM spect
PROBHD 5 mm CPTCI 1H/
PULPROG zg30
TD 65536
SOLVENT Acetone
NS 16
DS 2
SWH 12019.230 Hz
FIDRES 0.183399 Hz
AQ 2.7262976 sec
RG 32.25
DW 41.600 usec
DE 30.00 usec
TE 298.0 K
D1 1.00000000 sec
TD0 1
CHANNEL f1
SFO1 599.6637031 MHz
NUC1 1H
P1 8.35 usec
PLW1 6.30959988 W
F2 - Processing parameters
SI 65536
SF 599.6600101 MHz
WDW EM
SSB 0
LB 0.30 Hz
GB 0
PC 1.00

194PS_WaterAcetone2Aug

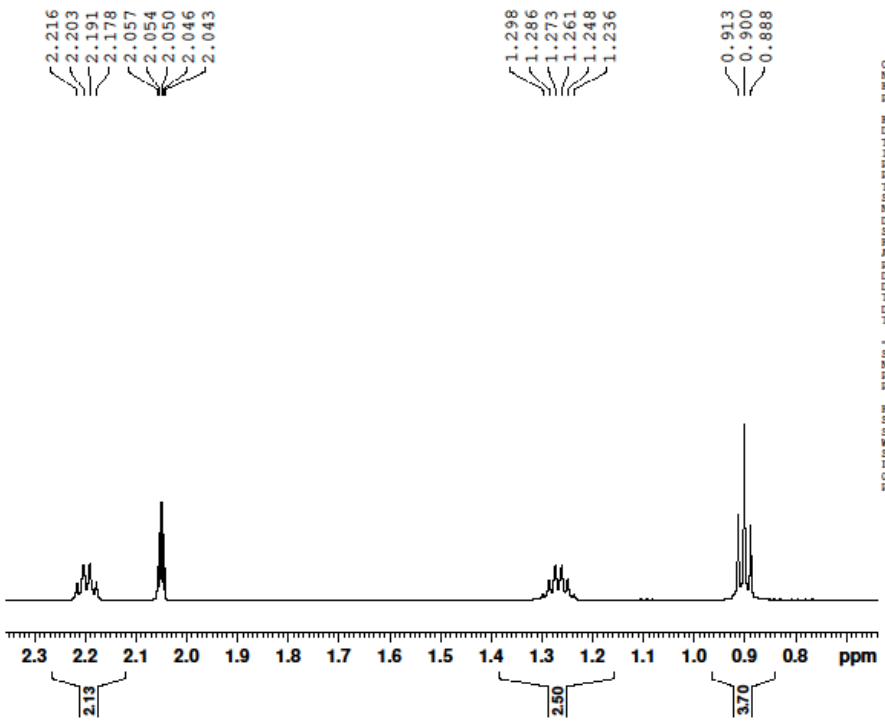


```
Current Data Parameters
NAME      194PS_WaterAcetone2Aug
EXPNO                          1
PROCNO                         1

F2 - Acquisition Parameters
Date_                   20180802
Time                       12.31
INSTRUM                    spect
PROBHD    5 mm CPTCI 1H/
PULPROG                     zg30
TD                         65536
SOLVENT                  Acetone
NS                              16
DS                               2
SWH                    12019.230 Hz
FIDRES                  0.183399 Hz
AQ                     2.7262976 sec
RG                          32.25
DW                         41.600 usec
DE                         30.00 usec
TE                         298.0 K
D1                     1.00000000 sec
TD0                              1

======== CHANNEL f1 ========
SFO1                599.6637031 MHz
NUC1                          1H
P1                         8.35 usec
PLW1                  6.30959988 W

F2 - Processing parameters
SI                         65536
SF                  599.6600101 MHz
WDW                           EM
SSB                0
LB                         0.30 Hz
GB                 0
PC                         1.00
```

NMRs of PgC_3 three hours after being dissolved in deuterated DMSO

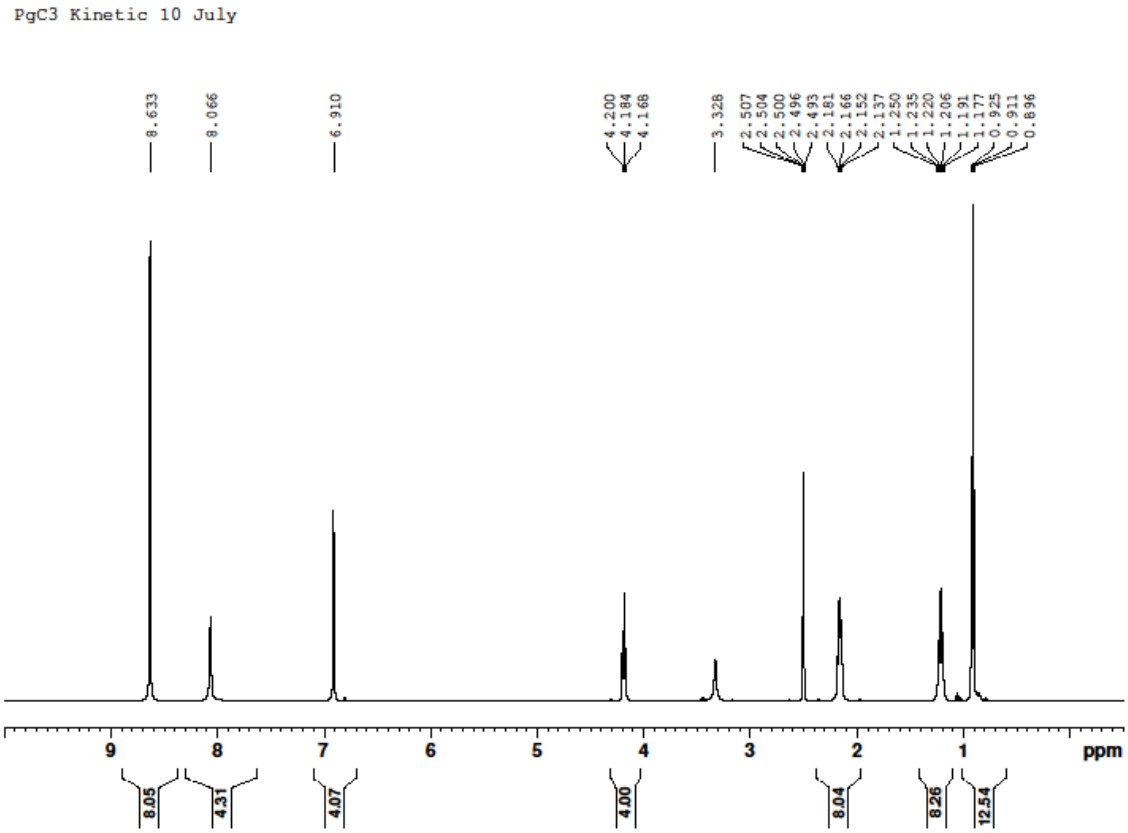

PgC3 Kinetic 10 July

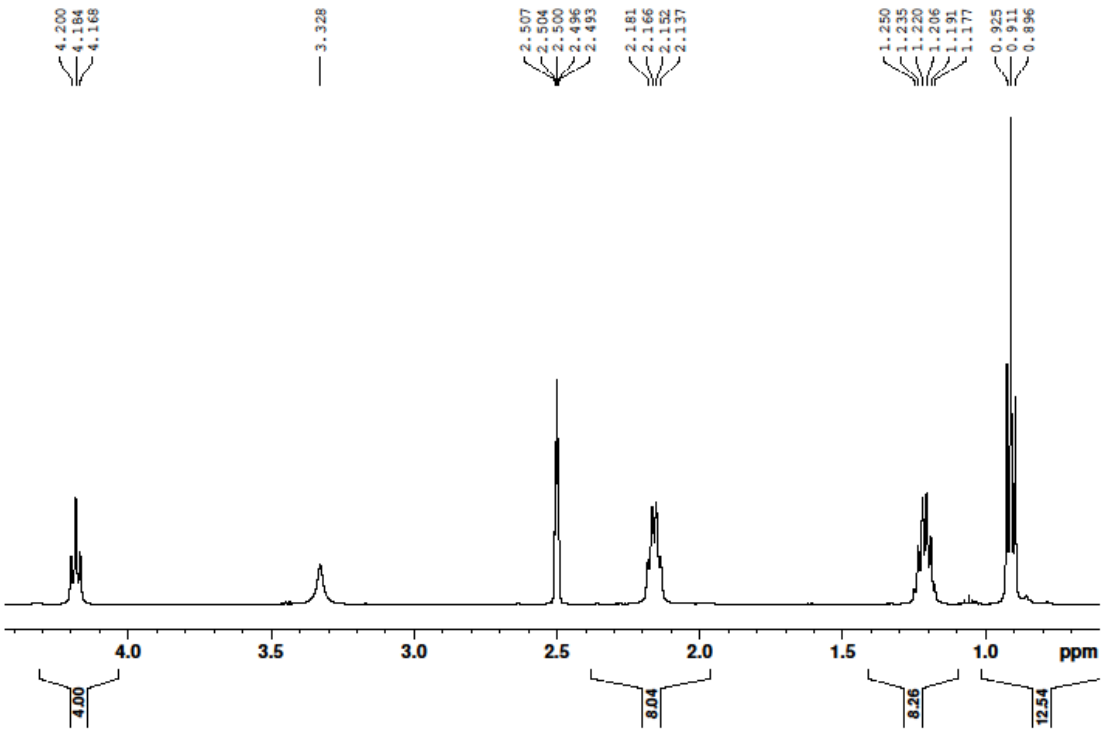

NMRs of PgC_3 five days after being dissolved in deuterated DMSO

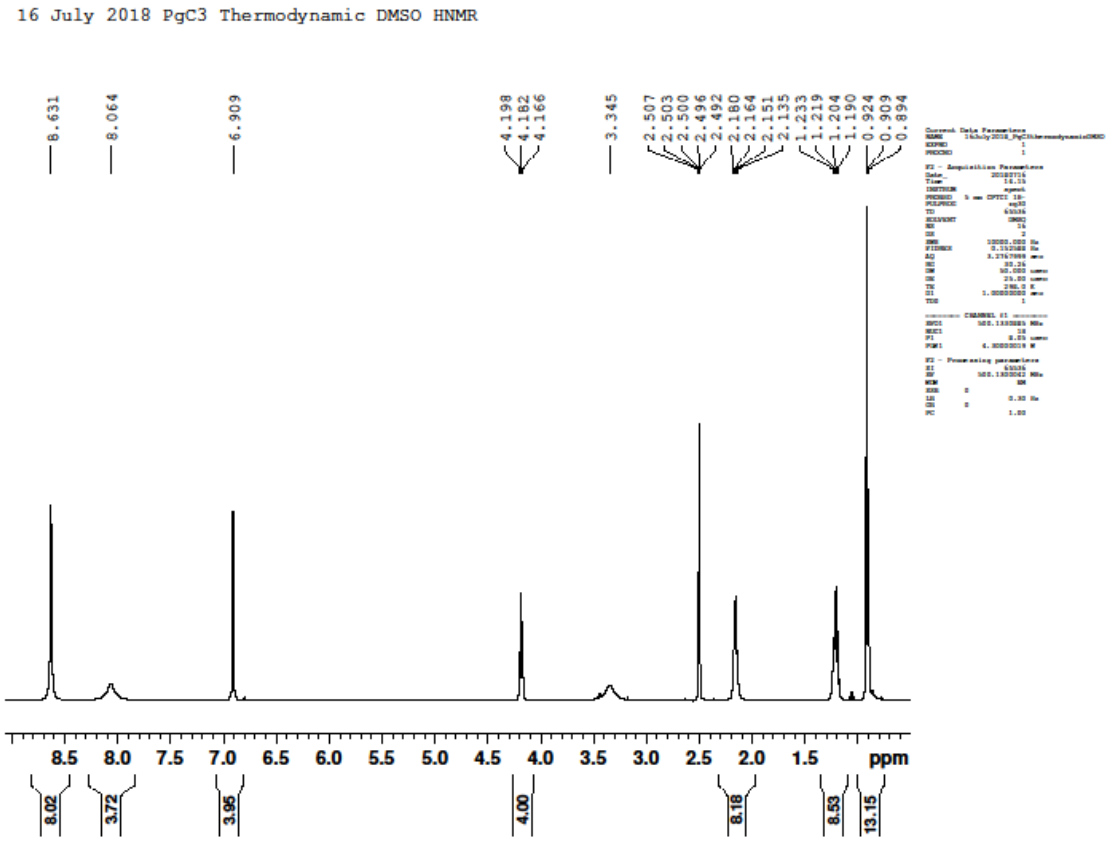

16 July 2018 PgC3 Thermodynamic DMSO HNMR

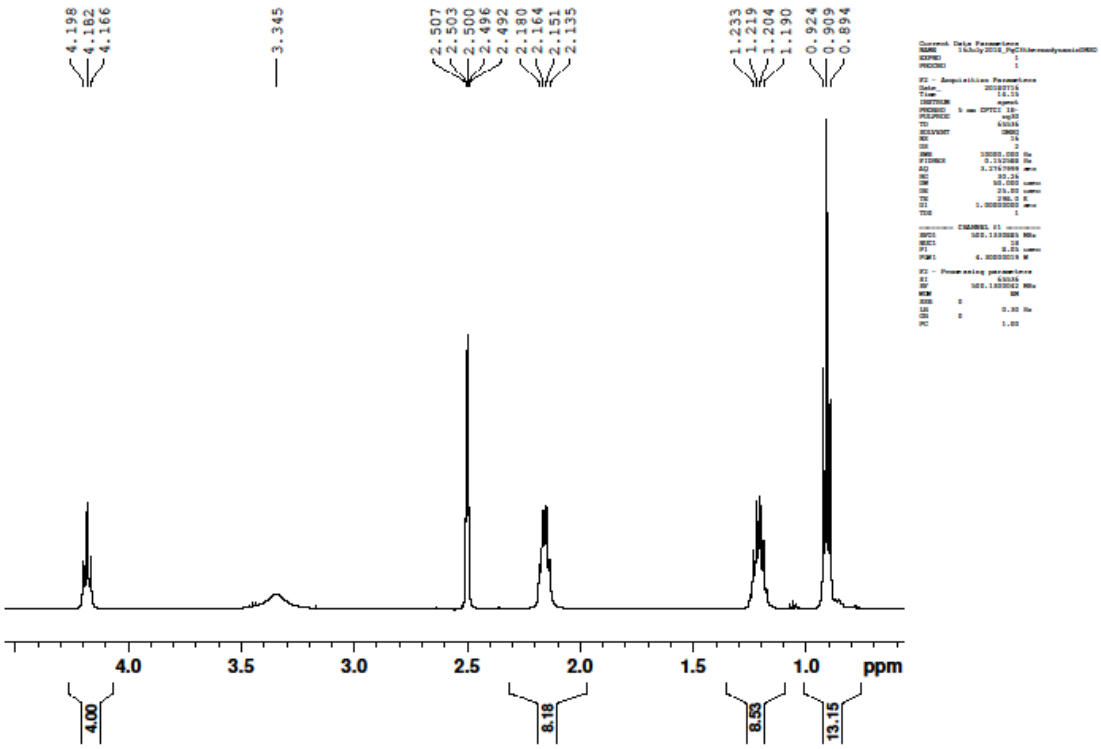

NMR of pyrogallol one hour after being dissolved in D_2O

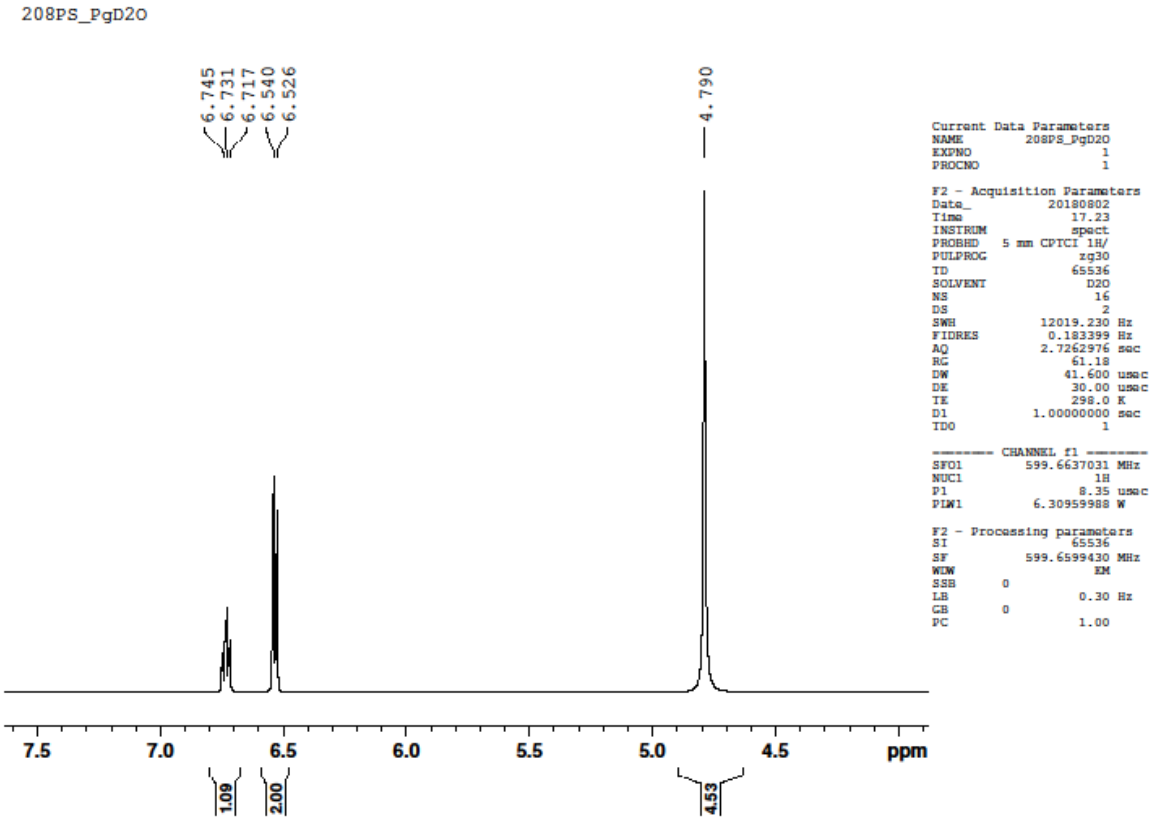

NMR of pyrogallol one month after being dissolved in D_2O

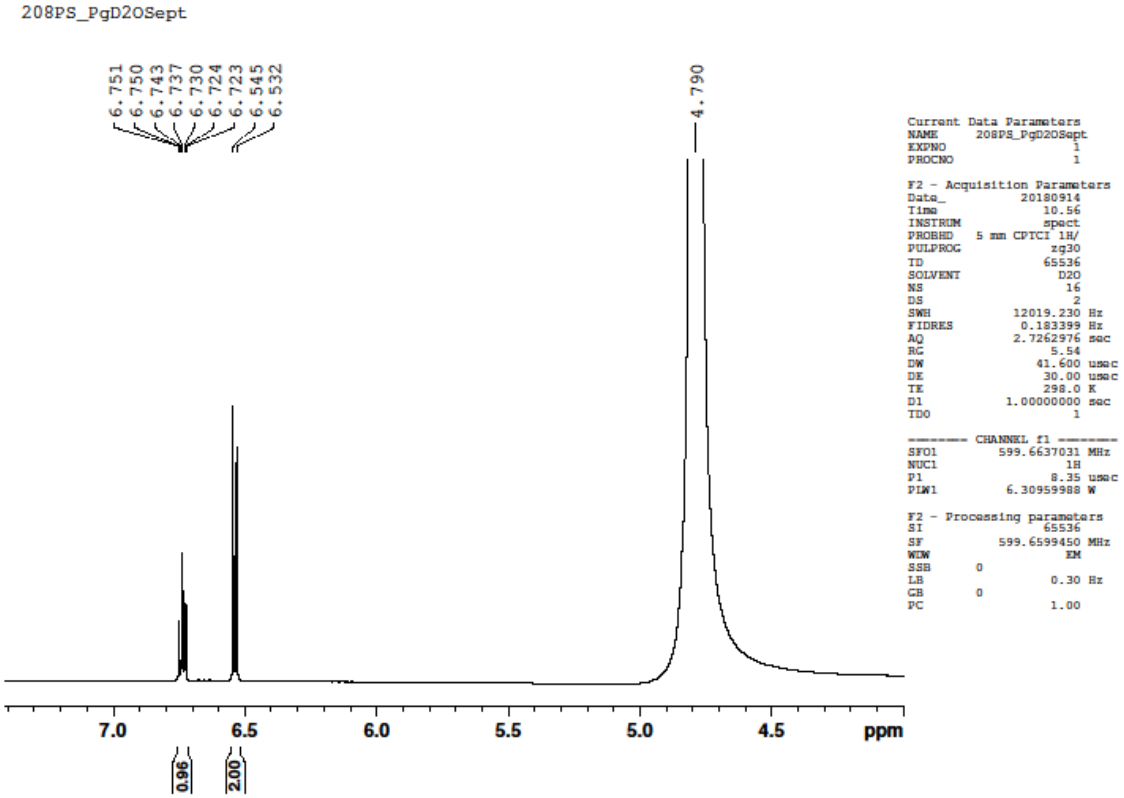

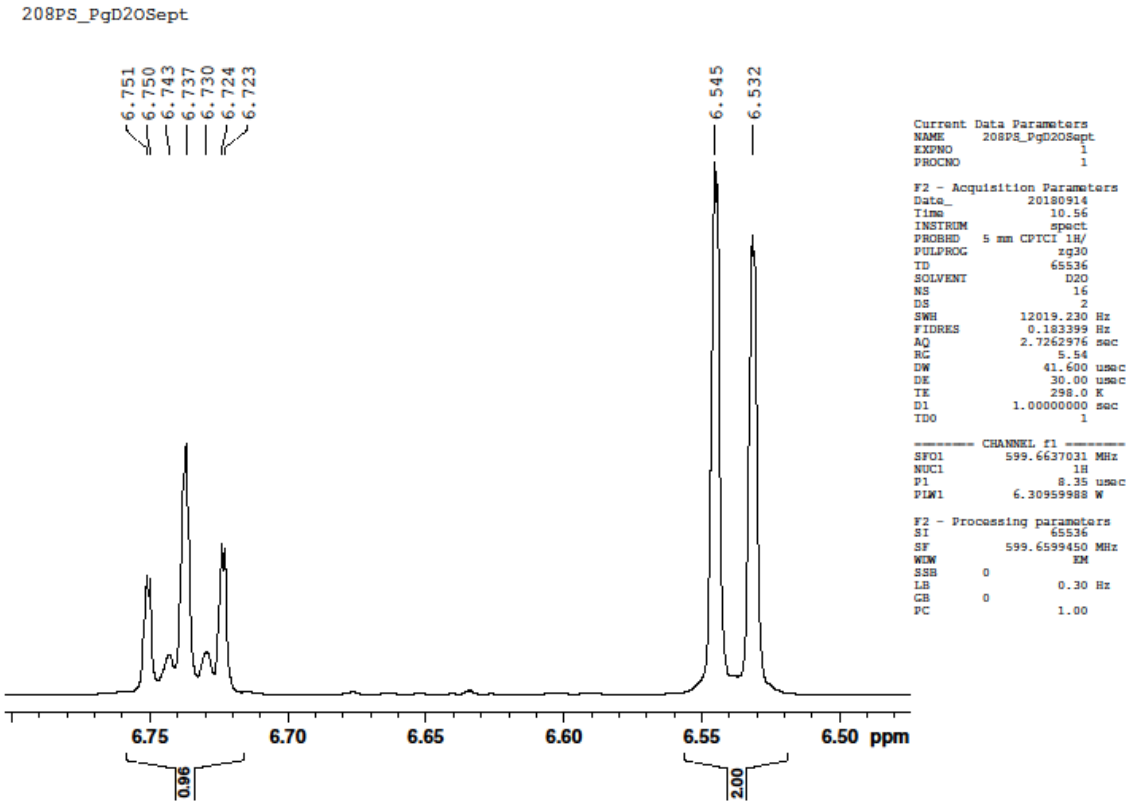
208PS_PgD2OSept
6.751
6.750
6.743
6.737
6.730
6.724
6.723
6.545
6.532
6.75
6.70
6.65
6.60
6.55
6.50 ppm
0.96
2.00
Current Data Parameters
NAME 208PS_PgD2OSept
EXPNO 1
PROCNO 1
F2 - Acquisition Parameters
Date_ 20180914
Time 10.56
INSTRUM spect
PROBHD 5 mm CPTCI 1H/
PULPROG zg30
TD 65536
SOLVENT D2O
NS 16
DS 2
SWH 12019.230 Hz
FIDRES 0.183399 Hz
AQ 2.7262976 sec
RG 5.54
DW 41.600 usec
DE 30.00 usec
TE 298.0 K
D1 1.00000000 sec
TD0 1
======== CHANNEL f1 ========
SFO1 599.6637031 MHz
NUC1 1H
P1 8.35 usec
PLW1 6.30959988 W
F2 - Processing parameters
SI 65536
SF 599.6599450 MHz
WDW EM
SSB 0
LB 0.30 Hz
GB 0
PC 1.00

VITA

PAUL SPIEL

919A Canterbury Dr. • Columbia, MO 65203 • spiel.paul@gmail.com • 208.569.8160

EDUCATION

University of Missouri, Columbia, MO
M.S. Chemistry (Dec. 2018)

- Adviser: Jerry Atwood
- Coursework: Organometallics, Organic Spectroscopy, Medicinal Chemistry, Biological Radiochemistry, Dissertation Research, Organic Reaction Mechanisms

Brigham Young University, J. Reuben Clark Law School, Provo, UT
Juris Doctor, April 2017

- Law Review, Lead Note and Comment Editor, 2016–2017
- Law Review, Associate Editor, 2015–2016
- 2017 John S. Welch Award for Outstanding Legal Writing, 2nd Place

Brigham Young University – Idaho, Rexburg, ID
Bachelor of Science, magna cum laude, Chemistry, July 2014

- GPA: 3.97
- Minor: Biology
- Relevant Coursework: Physical Chemistry, Inorganic Chemistry, Quantitative Analysis, Biochemistry, Organic Chemistry, Nuclear Chemistry, Physics, Calculus, Materials Science

EXPERIENCE

Atwood Lab, Columbia, MO
Graduate Research Assistant, Sept. 2017 – Present

- Investigating properties of calixarenes to advance knowledge of supramolecular chemistry and further nanocapsule development

United States Patent and Trademark Office, Denver, CO
Intern, June 2016 – Aug. 2016

- Conducted prior art searches, analyzed claims, and wrote office actions to expedite the examination of chemical patent applications (art unit 1755, solar cells)
- Aided a Patent Trial and Appeal Board judge in researching and writing an IPR decision

Pia Anderson Moss Hoyt, Salt Lake City, UT
Law Clerk, June 2015 – July 2015

- Drafted court documents and proposed claim construction to assist in a multimillion-dollar patent infringement dispute regarding Nintendo's Wii
- Read and evaluated scores of digital streaming patents to assess validity and licensing capabilities

Dabell Lab, Rexburg, ID
Research Assistant, Sept. 2013 – May 2014

- Successfully verified experimental results by employing methods of

computational chemistry to find low energy intermediates of radical reactions in the atmosphere

ADMISSIONS & PUBLICATIONS

Admissions:

- United States Patent and Trademark Office & Utah Bar

Publications:

- *Deceptive Patents: Deconstructing Juicy Whip*, 2017 BYU L. REV. 743 (2018)
- *Express Employee Patent Assignments: Staying True to Intellectual Property's Credo of Rewarding Innovation*, 99 J. PAT. & TRADEMARK OFF. SOC'Y 79 (2017)